Geological Society of America
Memoir 194
2001

Sedimentary and structural records of late Mesozoic high-strain extension and strain partitioning, East Gobi basin, southern Mongolia

Cari L. Johnson
Laura E. Webb*
Stephan A. Graham
Department of Geological and Environmental Sciences, Stanford University, Stanford, California 94305-2155, USA
Marc S. Hendrix
Department of Geology, University of Montana, Missoula, Montana 59812, USA
Gombosuren Badarch
Institute of Geology and Mineral Resources, Mongolian Academy of Sciences, P.O. Box 118, 63 Peace Avenue, Ulaanbaatar, Mongolia 210351

ABSTRACT

Contrasting styles of late Mesozoic sedimentation in the East Gobi basin of southern Mongolia in part reflect varying rates and structural modes of local extension. High-strain extension was associated with formation of an Early Cretaceous metamorphic core complex in the Onch Hayrhan area. Recent mapping illustrates newly recognized structural features of this core complex, including ductile structures that indicate subhorizontal south-southeast–directed extension ca. 126 Ma. A regionally extensive, east-west–trending detachment fault is locally domed, as defined by the rollover of foliation planes from north to south dipping. This detachment fault terminates to the east against a north-south–trending dextral strike slip transfer zone. Lower Cretaceous strata associated with this transfer zone are generally synextensional breccias and alluvial-fan deposits consisting of unsorted boulder conglomerate, interbedded debris-flow units, and rock-fall deposits that represent rapidly deposited components of proximal, syntectonic depositional systems. In contrast, several hundred kilometers to the northeast of this core complex late Mesozoic extension was characterized by more typical synrift structural geometries (e.g., high-angle normal faults bounding half-graben subbasins). Comparatively mature depositional systems represented by dominantly fluvial to lacustrine environments characterized the Early Cretaceous record in this part of the basin.

The combined structural and stratigraphic studies we present in this chapter demonstrate that the East Gobi basin was segmented into regions of high- and low-strain extension, and that transfer zones accommodated these variations. In southern Mongolia and other parts of central Asia, late Mesozoic metamorphic core complex formation is typically associated with a rapid transition from compressional to extensional tectonics, particularly along orogenic belts associated with convergent terrane and plate margins.

*Current address: Department of Earth Sciences, 204 Heroy Geology Laboratory, Syracuse University, Syracuse, New York 13244-1070, USA

Johnson, C.L., et al., 2001, Sedimentary and structural records of late Mesozoic high-strain extension and strain partitioning, East Gobi basin, southern Mongolia, *in* Hendrix, M.S., and Davis, G.A., eds., Paleozoic and Mesozoic tectonic evolution of central Asia: From continental assembly to intracontinental deformation: Boulder, Colorado, Geological Society of America Memoir 194, p. 413–433.

This implies that gravitational collapse along tectonic boundaries may have played an important role in the localization of high-strain extension throughout the region.

INTRODUCTION

Mesozoic sedimentary basins of eastern China have long been recognized as a group of intracontinental rift basins (Watson et al., 1987). They are distinct from many of the basins of western China that are associated with Mesozoic compression (collisional successor basins of Graham et al., 1993; Fig. 1). Extension commenced in the Late Jurassic to Early Cretaceous in north-central China, (e.g., Erlian Basin; Li Chansong et al., 1997), younging eastward to the Tertiary offshore basins (e.g., Bohai Bay; Watson et al., 1987). This extensional regime has also been recognized in the Tamsag and East Gobi basins of eastern Mongolia, which are contiguous with Hailar and Erlian basins, respectively (Shuvalov, 1975; Traynor and Sladen, 1995; Fig. 1).

Many important aspects of these rift basins remain poorly documented, including the magnitude, style, and kinematics of extension, as well as details of sedimentary fill patterns. Furthermore, sedimentary studies of rift basins in central Asia have raised several important regional questions, including what factors may have driven extension, and how these basins may relate to documented early Mesozoic compression (Graham et al., 1996; Hendrix et al., 1996; Davis et al., 1998b; Dumitru and Hendrix, this volume).

In order to better understand late Mesozoic basin evolution, we focused on mapping the structure and the sedimentary and volcanic basin fill of the East Gobi basin of southern Mongolia. Previously, we documented the existence of the Cretaceous Yagan–Onch Hayrhan metamorphic core complex at the southwestern edge of the basin, along the China-Mongolia border (Webb et al., 1999; Fig. 2). Our regional studies indicate that two fundamentally different styles or end members of extension occurred in the East Gobi basin during Early Cretaceous time: (1) high-strain detachment faulting in the southwest, and (2) rifting and half-graben formation in the northeast. The differences in strain may be accommodated by transfer zones similar to the strike slip shear zone at Onch Hayrhan, as well as possibly unrecognized accommodation zones in other parts of the basin. In this chapter, we present new data from the Yagan–Onch Hayrhan core complex, briefly review the sedimentary record of rifting in the East Gobi basin, and consider the differences in extensional style within the context of basin-scale and regional-scale strain partitioning.

Geology of the East Gobi basin

The East Gobi basin is a northeast-southwest–oriented elongate basin that is divided into a series of fault-bounded subbasins, including most notably the petroliferous Unegt and Zuunbayan subbasins (Fig. 2). Northwest-southeast–trending faults and sediment-covered corridors interrupt the northeast-southwest strike continuity of rift structures and further partition Mesozoic sedimentary depocenters. Along its southern margin, the East Gobi basin is separated from the Erlian basin in China by an uplifted block of Precambrian–Paleozoic basement rocks (the Toto Shan block of Zonenshain et al., 1971) and by the Zuunbayan fault (Fig. 2; Suvorov, 1982).

Although little is known about the Zuunbayan fault, late Cenozoic strike slip fault activity is well documented in several areas of western and central Mongolia (Cunningham et al., 1997; Baljinnyam et al., 1993). Recent models of the Mesozoic–Cenozoic tectonic evolution of Mongolia have featured differing interpretations of the timing of initial fault activity (cf. Lamb et al., 1999; Yue and Liou, 1999). Proprietary seismic reflection data confirm a component of dip-slip normal faulting along the Zuunbayan fault zone during the Early Cretaceous, although strike slip faulting may have also played an important role in Mesozoic basin formation.

A series of Late Jurassic normal faults, reactivated as reverse faults during mid-Cretaceous compression, generally define the northern margin of the East Gobi basin (Suvorov, 1982; Traynor and Sladen, 1995), although detailed mapping of this margin is not currently available. To the south and east, the East Gobi basin extends into China and is generally contiguous with the northern edge of the Erlian basin (Fig. 2). To the southwest, it becomes a region of high-strain extension typified by the Yagan–Onch Hayrhan core complex (Zheng and Zhang, 1993).

Rifting in the East Gobi basin began in Late Jurassic time; as much as 2–3 km of nonmarine synrift sediment and volcanic flows fill asymmetric half-grabens (Fig. 3A; Graham et al., 1996). Widespread mid-Cretaceous uplift, possibly related to transpression, inverted the synrift sequence along the basin margins. Typically flat-lying Upper Cretaceous strata unconformably overlie tilted synrift strata (Fig. 3B; Traynor and Sladen, 1995), signaling the end of Mesozoic tectonism (Shuvalov, 1968).

MESOZOIC HIGH-STRAIN EXTENSION IN THE ONCH HAYRHAN REGION

Structure of the Yagan–Onch Hayrhan metamorphic core complex

The Yagan–Onch Hayrhan metamorphic core complex (Fig. 2) was first recognized in China by Zheng et al. (1991), and its continuation into southern Mongolia was documented by Webb et al. (1997, 1999). Its classic core complex components grade structurally upward from a plutonic and gneissic core, through an ~1-km-thick mylonite zone, to a topographically well-expressed detachment fault with a 5–10-m-thick chloritic breccia zone (Webb et al., 1999). Kinematic indicators from ductile and brittle structures indicate south-southeast–directed subhorizontal extension, consistent with the overall trend of the East Gobi basin. Synkinematic biotite yielded $^{40}Ar/^{39}Ar$ ages ranging from 129 to 126 Ma (Webb et al., 1999). This Early Cretaceous age of deformation closely corresponds with the age of

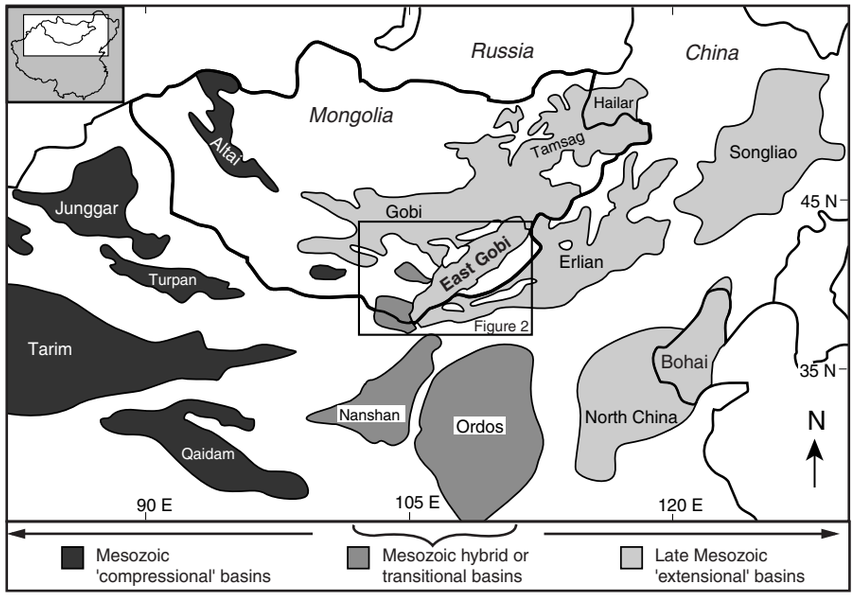

Figure 1. Mesozoic sedimentary basins of central Asia. Basins are generally divided into western basins formed by contractional tectonics during Triassic–Jurassic, eastern basins formed during Jurassic–Cretaceous intracontinental rifting, and hybrid or transitional basins with multiphase, transtensional and/or transpressional tectonic histories (modified from Watson et al., 1987).

volcanic tuffs and basalt sequences preserved in the basin (Shuvalov, 1968; Keller and Hendrix, 1997; Johnson et al., 1997a).

Following the initial results of Webb et al., 1999, we completed more detailed mapping on 1:100 000-scale topographic maps and 1:20 000-scale aerial photographs. Geologic transects included mapping, measurement, and documentation of foliations, lineations, faults and/or shear zones and folds, and their relative ages and types (Figs. 4 and 5). Shear sense was determined from *schistositi-cisaillement* fabrics, shear bands, and offset features. In domains of homogeneous deformation, shear sense was assessed from rotated and/or asymmetric features such as sigma and delta clasts. Mesoscopic fault-slip data were collected to understand fault arrays. The orientation and sense of slip on faults was used to calculate principal stress orientations and shape factors, qualitatively describing the stress geometry (Fig. 6). See Angelier (1994) and Passchier and Trouw

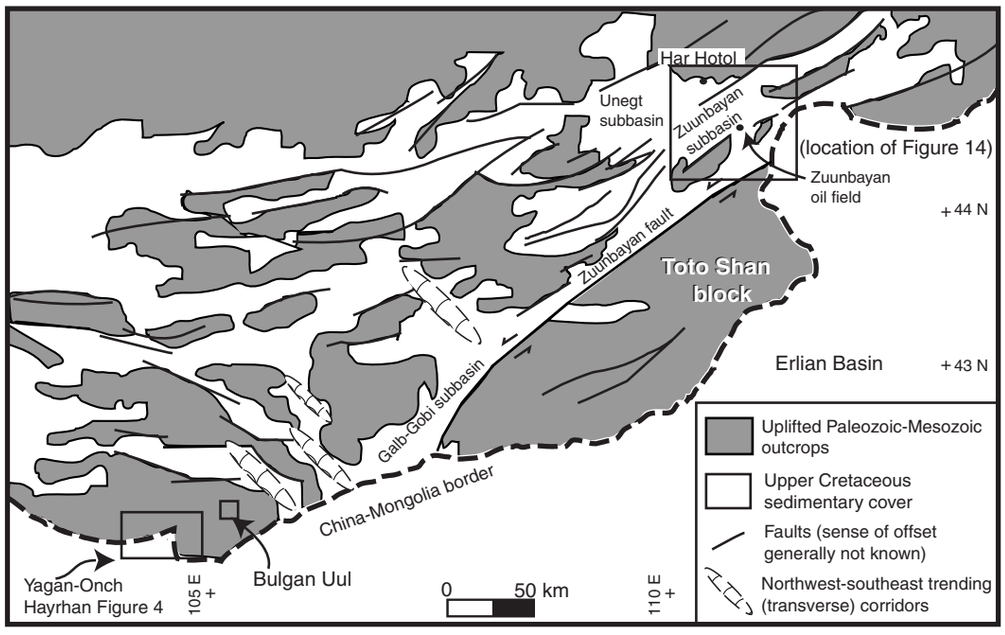

Figure 2. Generalized structure of East Gobi basin. Shaded areas represent uplifted regions with outcrops of Paleozoic–Lower Cretaceous strata separating fault-bounded subbasins. Overall northeast-southwest–oriented structural grain of basin is further subdivided by northwest-southeast–trending sediment-covered corridors.

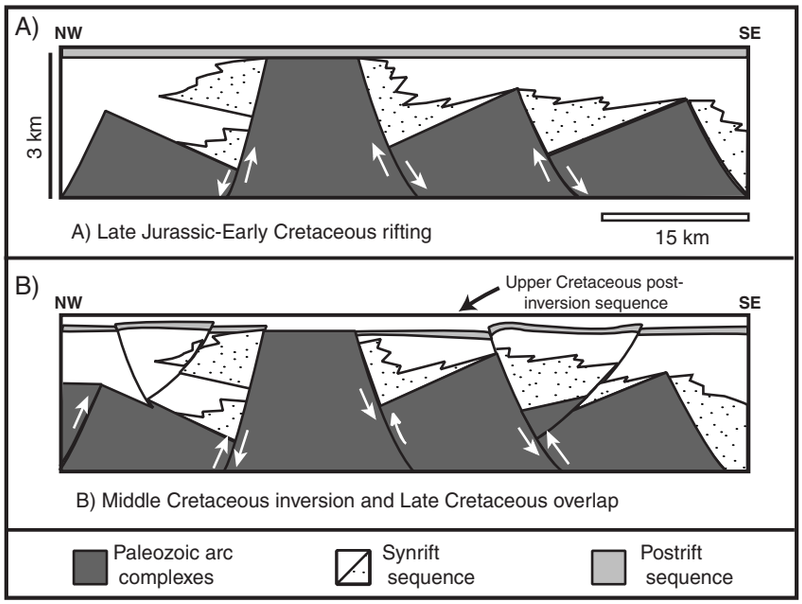

Figure 3. Schematic evolutionary cross sections of northeastern part of East Gobi basin near Zuunbayan (Fig. 2). Modified from Traynor and Sladen (1995). Cross sections are shown for rift development stage (A) and postrift inversion and overlap stage (B).

(1996) for comprehensive summaries and critical discussions of these structural methods.

We now present new field and structural data from the Yagan–Onch Hayrhan core complex (Figs. 4–6) concerning: (1) older ductile features that are overprinted by structures associated with south-southeast–directed extension and intruded by inferred Early Cretaceous plutons; (2) the northward rollover of the south dipping detachment into north-dipping foliation; and (3) a dextral transfer fault that forms the eastern boundary of the core complex and includes a series of high-angle brittle normal fault splays branching eastward.

Pre-core complex structures. The northern zone of the Onch Hayrhan core complex comprises a northeast-trending swath of metasedimentary rocks including interbedded stretched-pebble conglomerate, metasandstone, slate, and limestone (Fig. 4). The level of metamorphism decreases to the northeast from chloritic greenschist facies in the core of the complex to a relatively undeformed, unmetamorphosed sedimentary protolith section. This sequence of interbedded carbonate, conglomerate, sandstone, and shale is strikingly similar to Lower Permian rocks exposed at Bulgan Uul, ~30 km northeast of Onch Hayrhan Mountain (Ruzhentsev et al., 1989; Pavlova et al., 1991; Fig. 2). Both sections are distinctly different from outcrops of Carboniferous–Devonian arc-related marine sedimentary rocks in the area (Lamb and Badarch, 1997), and they bear no resemblance to the poorly lithified, proximal, synextensional conglomerate units of the Lower Cretaceous.

Foliations in the metasedimentary rocks typically dip steeply to the southeast (Fig. 5), although localities with consistent dips of almost every orientation were observed (Fig. 6, group i). Stretching lineations plunge moderately to subhorizontally southwest or northeast. In the higher grade and more strongly deformed sections of these rocks, shear sense is nearly universally top-to-the-southwest. However, two localities with top-to-the-northeast shear sense (Fig. 6, group i, plots I and J) were observed. Southward toward the detachment, tension gashes indicating northwest-southeast subhorizontal extension become increasingly abundant and crosscut the fabrics related to top-to-the-southwest shearing (Fig. 6, group ii). These metasedimentary rocks are also intruded by undeformed dikes and plutons of inferred Early Cretaceous age, and are in normal fault contact with Lower Cretaceous sedimentary rocks (Figs. 4, 5, and 7; Webb et al., 1999).

Thus, the top-to-the-southwest shear-sense indicators appear to be overprinted by younger shear indicators associated with Early Cretaceous northwest-southeast detachment faulting. Furthermore, top-to-the-southwest structures observed in the northern part of the Onch Hayrhan locality underlie Precambrian(?) carbonate and quartzite klippen (Figs. 4 and 8). These klippen are inferred to be the remnants of a large fold and thrust belt emplaced during Jurassic time (Zheng et al., 1991, 1996; Webb et al., 1999). We propose that the age of the southwest-oriented shear deformation in the metasedimentary units is bracketed between Permian (age of protolith sedimentary section) and Early Cretaceous (age of crosscutting features), and may be related to contractional deformation prior to core complex formation.

Domal structure. In the high-grade region of the core complex south of the metasedimentary section described here, foliations in schist and gneiss dip gently to the north-northeast, and stretching lineations plunge moderately to subhorizontally to the northwest (Figs. 4 and 6, group iii, plots A–D). These fabrics gradually rollover within a zone of ~1 km into southwest- and southeast-dipping foliations and southeast-plunging lineations associated with the detachment fault along the southern boundary of the core complex (Figs. 5 and 6, group iii, plots E

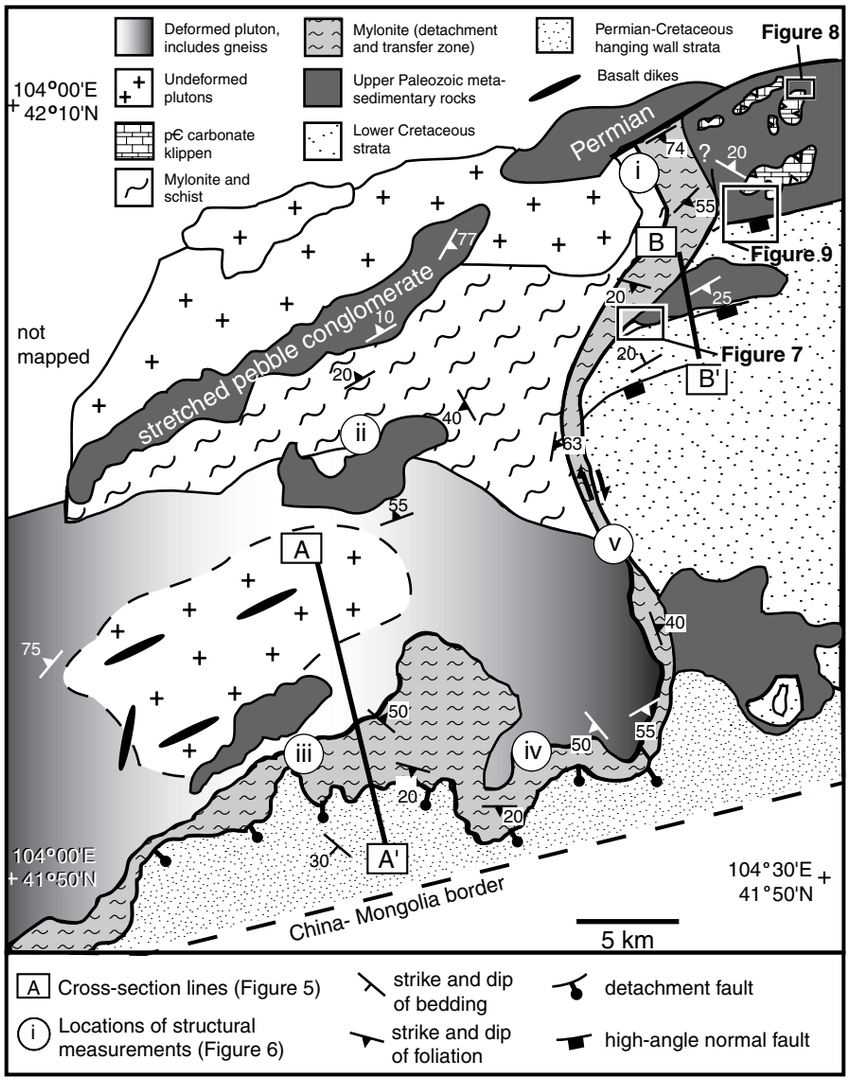

Figure 4. Outcrop structure of Onch Hayrhan region, including locations of cross sections (Fig. 5), structural measurements (Fig. 6), field photographs (Figs. 7 and 8), and sedimentary observations (Fig. 9).

and F, and group iv). Shear sense is uniformly top-to-the-southeast. This domal feature dies out eastward along the detachment, which has only south dipping foliation as it approaches the transfer fault (Figs. 4 and 5).

Transfer zone and brittle structures. From where it first crosses the border from China into Mongolia, the south dipping detachment surface can be traced eastward along strike for ~30 km (Fig. 4). At the point where the domal feature dies out, the detachment changes abruptly into a north-south–trending dextral shear zone. The shear zone is ~100 m wide, and separates mylonitic rocks of the core complex from a Lower Cretaceous sedimentary section to the east (Fig. 7). The transfer fault can be traced north from the detachment for ~15 km. Along its length, a series of brittle normal faults splay off to the east until the transfer zone dies out to the north (Figs. 4 and 7). Principal stress directions computed for the fault-slip data at localities within the transfer zone indicate that deformation was associated with subhorizontal south-southeast extension (Fig. 6, group v), and is identical to the extension direction indicated by stretching lineations in the metamorphic footwall.

Following the terminology of Faulds and Varga (1998), this feature can be classified as a dextral synthetic transfer, similar in geometry to the Las Vegas Valley shear zone of the western United States (Duebendorfer and Wallin, 1991). This dextral transfer zone is a key feature, in that it is among the structures that accommodate the transition from the high-strain extensional province of the Yagan–Onch Hayrhan core to a lower strain extensional province of the East Gobi basin.

Discussion. These new observations strengthen the interpretation of the Onch Hayrhan area as a metamorphic core complex. This region shares many similarities with classic examples from the western United States (Coney, 1980), including a domal, gently dipping detachment zone that juxtaposes ductile fabrics in mid-crustal rocks of the lower plate with relatively

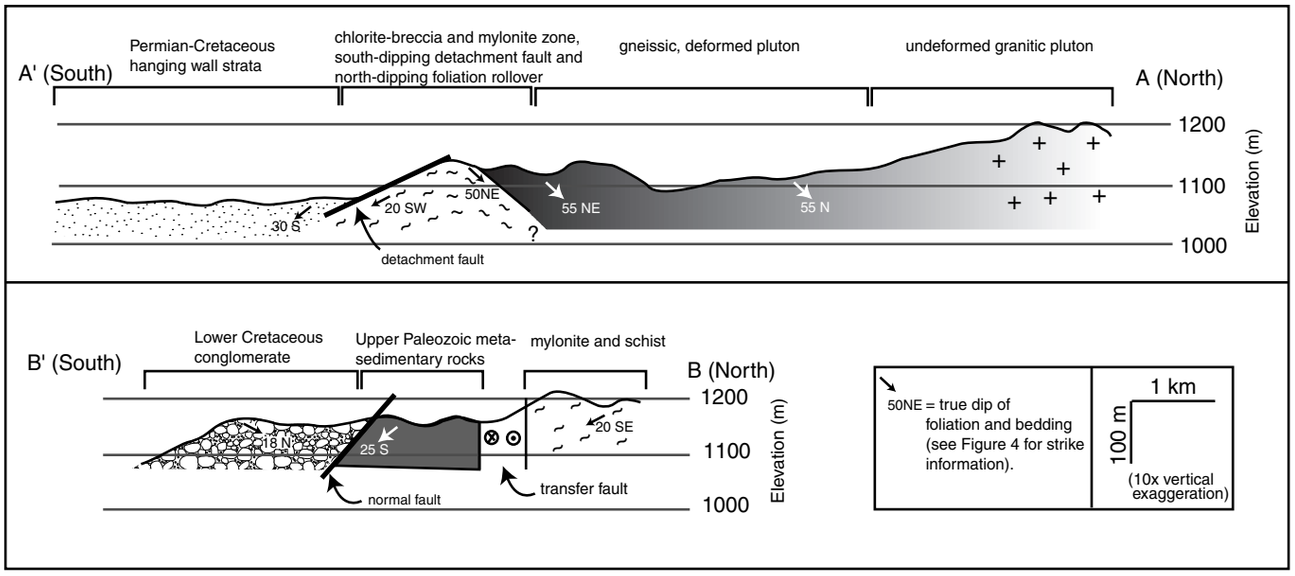

Figure 5. Cross-sections A′-A and B′-B (see Fig. 4 for location). Note domal structure of mylonitic foliation along detachment fault (A′-A), and high-angle normal fault that downdrops synextensional Lower Cretaceous conglomerate against Paleozoic basement rocks (B′-B). Detailed structural data are shown in Figure 6.

unmetamorphosed upper plate rocks, and termination of the detachment fault against a transfer zone oriented obliquely to the extension direction. The Early Cretaceous age of extension (Webb et al., 1999) implies that high-strain extension played a major role in controlling basin structure in parts of the Cretaceous East Gobi basin.

In addition, most of the crystalline rocks associated with this core complex were originally mapped as Precambrian (Yanshin, 1989) and were thought to represent part of the South Gobi microcontinent (Şengör et al., 1993). Although we cannot yet entirely discount the possibility of a Precambrian protolith in southern Mongolia, our field work indicates that the main protoliths at Onch Hayrhan are likely to be upper Paleozoic metasedimentary rocks. We currently are testing this hypothesis by sensitive high–resolution ion microprobe (SHRIMP) analyses of zircons in order to establish protolith ages of metamorphic rocks from Onch Hayrhan and other East Gobi basin localities. Preliminary results indicate that Onch Hayrhan protoliths are younger than Precambrian (T. Cope, 1999, personal commun.). This work further supports the idea that the crust of southern Mongolia is exclusively a collage of Paleozoic arc complexes accreted during the middle to late Paleozoic (Lamb and Badarch, 1997).

Field observations also suggest the existence of an older, overprinted deformation represented by top-to-the-southwest features found north of the detachment fault. In the northeast, these features underlie large carbonate and quartzite klippen (Fig. 8). Similar Triassic–Jurassic thrust-sheet remnants have been reported along the Chinese side of the border (Zheng et al., 1996). Other evidence of early Mesozoic compression includes inferred Permian–Jurassic foreland basin strata northwest of Onch Hayrhan at Noyon Uul (Hendrix et al., 1996, this volume; Dumitru and Hendrix, this volume), and concurrent thrust faulting in Inner Mongolia (Davis et al., 1998c; Darby et al., this volume). Thus, we propose that the overprinted top-to-the-southwest structures may record a compressional precursor to extension.

Sedimentary record of high-strain extension

Lower Cretaceous sedimentary rocks associated with the Onch Hayrhan core complex crop out east of the transfer zone in a series of discrete subbasins bounded by high-angle normal faults that offset upper Paleozoic (Permian) metasedimentary rocks (Figs. 7 and 9). Although no volcanic layers have yet been found within the sedimentary section, the remarkably coarse grained, proximal nature of the deposits strongly suggests a synextensional origin. In addition, the conglomerate contains clasts of upper Paleozoic sedimentary rocks of the hanging wall, as well as granite, gneiss, and mylonite lithologies found within the footwall of the core complex. The north-dipping conglomerate is overlapped by relatively flat lying Upper Cretaceous clastic rocks that form the postrift sedimentary cover throughout southern Mongolia. Thus, this sedimentary sequence postdates core complex metamorphism and predates the overlap sequence, which generally is early Cenomanian at its base in southern Mongolia (Jerzykiewicz and Russell, 1991). Based on its syntectonic character, we infer that the Lower Cretaceous

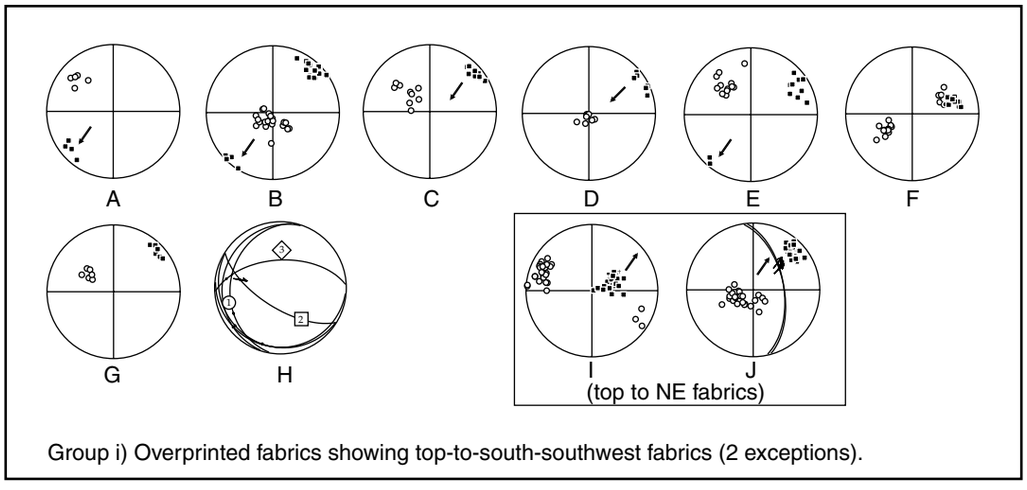

Figure 6. Stereonets of kinematic indicators from brittle and ductile fabrics, locations (i–v) in Figure 4. Shear sense in older fabrics (group i) is generally top to southwest, and is overprinted by top to southeast fabrics related to detachment faulting (groups ii to iv), and by oblique dextral slip indicators near transfer fault (group v).

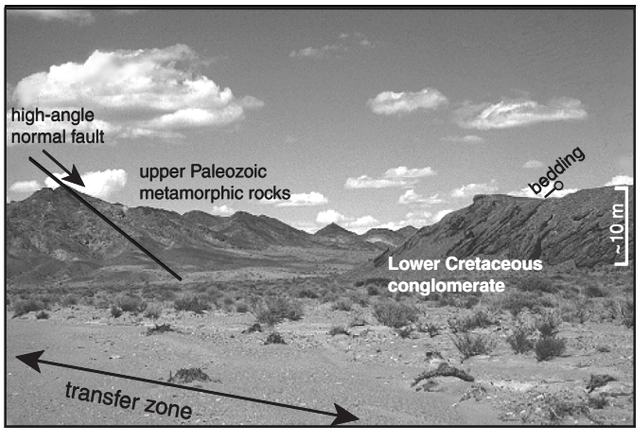

Figure 7. Photograph looking east across north-south–trending transfer zone. Transfer fault is exposed just west of frame of view, and extends northward, parallel to drainage shown in picture (see Fig. 4 for location). East-west–trending high-angle normal fault downdrops Lower Cretaceous conglomerate sequence against upper Paleozoic metamorphic rocks.

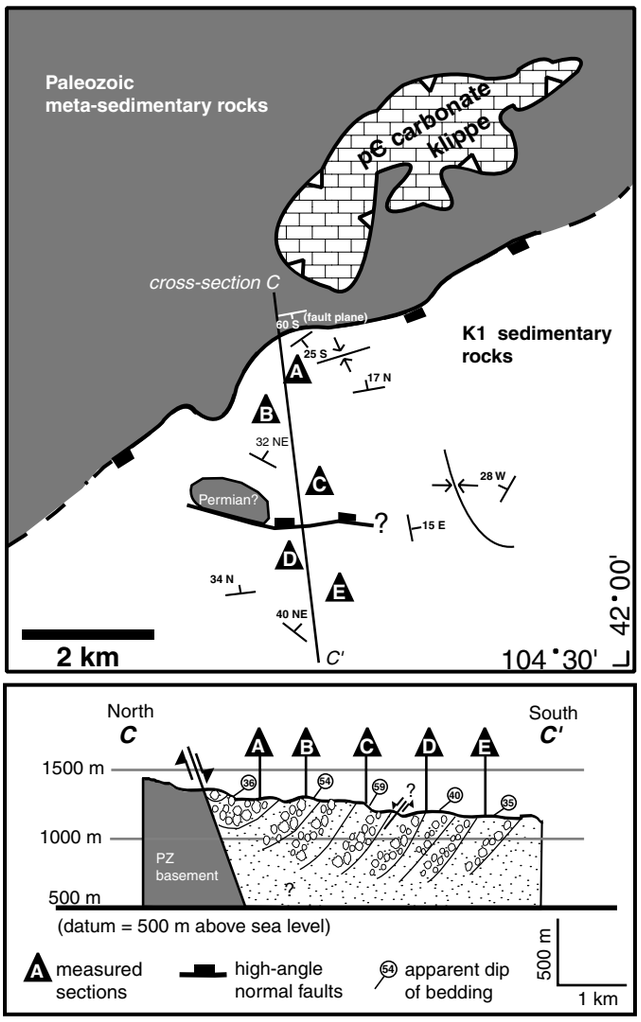

Figure 9. Location and structure of Lower Cretaceous sedimentary section. Locations of detailed measured sections (Fig. 10) are shown by black triangles. Black strike and dip symbols are bedding orientations. See Figure 4 for location.

sequence formed during and/or immediately following high-strain extension ca. 126 Ma.

A complete measured stratigraphic section is not possible due to the formation of separate half-graben depocenters, the possibility of offlapping stratigraphic shingling (cf. Crowell, 1974), and intermittent exposures. Although not continuous, exposure is superb locally, and we chose to measure a series of smaller sections at decimeter resolution in order to typify depositional style and detrital composition (Figs. 9 and 10). Based on structural and facies relations, we are able to place these measured sections in their relative stratigraphic positions in Figure 10. The section is disrupted by a covered interval and a minor antithetic normal fault between sections C and D (Fig. 10); however, the reconstructed composite section provides a sense of minimum thickness of the basin fill, and permits inferences about the evolution of the extensional system and Early Cretaceous landscape.

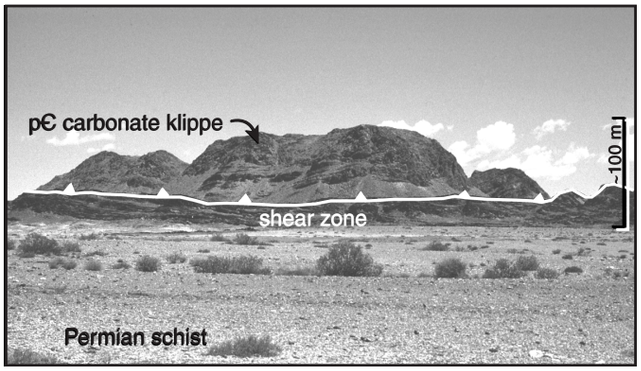

Figure 8. Photograph of large klippe of Precambrian carbonate overlying Permian and upper Paleozoic schist across flat thrust-fault contact. See Figure 4 for location.

Lower Cretaceous facies. Lower Cretaceous strata are exposed east of the transfer zone, adjacent to and rotated toward high-angle normal faults that offset Paleozoic basement (Figs. 7 and 9). Bedding dip angles increase slightly in the older units, indicating progressive fault activity and bed rotation during deposition (Fig. 9: cross section and measured sections A–C). The sedimentary sequence mainly consists of coarse-grained (clasts commonly 0.25 to >1 m diameter), poorly sorted, cobble to boulder conglomerate that indicates proximal, rapid, synextensional deposition. Boulders of Paleozoic crinoidal limestone testify to the proximal nature of these deposits, because meter-scale boulders of coarsely crystalline carbonate would not have

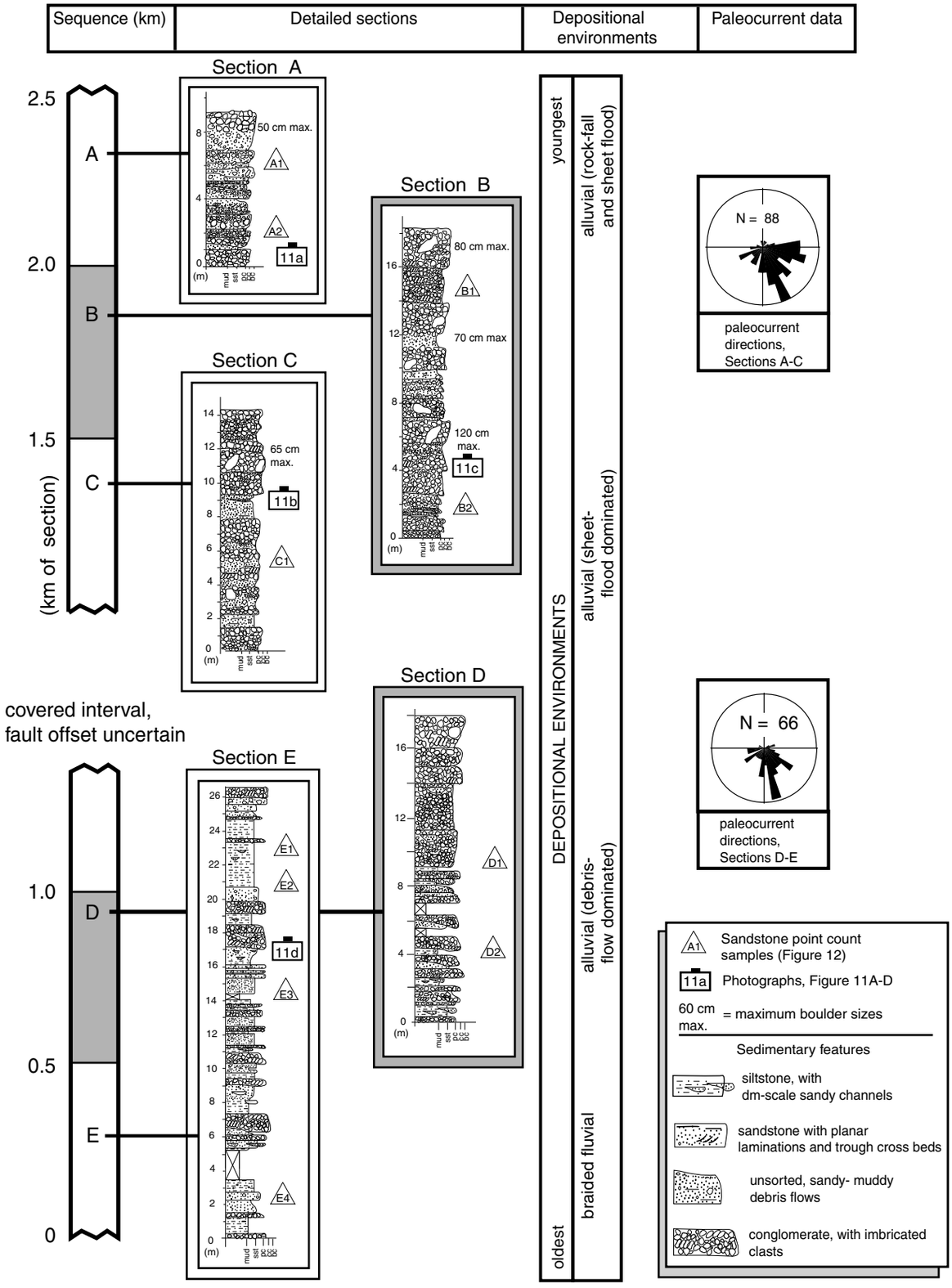

Figure 10. Detailed stratigraphic sections from Lower Cretaceous transect shown in Figure 9. Sections are shown in their approximate stratigraphic positions relative to overall sequence (left column), although thickness missing between sections C and D is not certain. All paleocurrent data are from pebble imbrication measurements. Vertical scales are same for all sections. Grain-size scale: mud, mudstone/siltstone; sst, sandstone; pc, pebble conglomerate; cc, cobble conglomerate; bc, boulder conglomerate.

survived transport over distances of more than a few kilometers. Paleocurrent directions from imbricated clasts are directed toward the south-southeast throughout the section (Fig. 10), indicating drainage from the footwall blocks of half-grabens within the Paleozoic basement.

Sedimentary facies are characteristic of alluvial fan deposits, and can be divided into three general categories following the terminology of Blair and McPherson (1994). These groups are defined as rock-fall units, debris flows, and sheetflood deposits, in order of increasing abundance in the section.

Rock-fall units are represented by unsorted, clast-supported, extremely coarse deposits of angular boulders with very little matrix (Fig. 11A). These preserved talus cones are ~10 m in lateral width (i.e., cone diameter). They are rare in the section, and likely are formed due to slope failure along steep fault scarps (Beratan, 1998). Larger rock slides and rock avalanches were not observed, though they may have been transported further into the basin, thus bypassing the proximal fan deposits.

Debris-flow beds are present as matrix-rich, internally unorganized planar beds up to 2 m thick. Matrix ranges from sandy to clayey, and beds are unsorted, with floating, cobble-sized angular clasts (Fig. 11B). Debris-flow units are locally erosive at their bases, and also show reworking of the upper parts of the underlying bed. These are interpreted as cohesive, hyperconcentrated, and high-density flows formed by slope failure in water-saturated colluvium. The debris flows are most common in the upper parts of the sequence (Fig. 9, sections A–C), where they are interbedded with clast-supported conglomerate beds interpreted as sheetflood units (Blair and McPherson, 1994).

Sheetflood deposits constitute most of the volume of the Lower Cretaceous strata. Bed thicknesses range from 0.5 m to >2 m, and include interbedded coarse conglomerate and sandier units. Most typically, conglomerate beds display crude to well-defined stratification, erosional channelization, and clast imbrication, indicating some degree of water working and bed-scale traction structures (Fig. 11C). Smaller scale structures (e.g., ripples, cross-beds) are rare, but in overall finer grained intervals, conglomerate with better rounded pebbles occurs in thin channel-form lenses encased in plane- to cross-laminated sandstone. Grain-supported conglomerate beds display both upward-coarsening and upward-fining trends, and are frequently interbedded with matrix-supported unstratified to poorly stratified pebbly mudstone and sandstone.

In addition to the alluvial facies described here, the lower part of the section (typified by detailed section E, Fig. 10) displays finer grained, pervasively channelized, imbricated, and rounded pebble to cobble conglomerates (Fig. 11D). The section also contains fine-grained, mottled, oxidized units interpreted as possible overbank or bar-top deposits and paleosols. In contrast to the rest of the sequence, which is dominated by alluvial processes and flash-flood, episodic sedimentation, these facies are interpreted as representing a seasonal braided stream environment.

Conglomerate and sandstone provenance. We collected compositional data from the sandstone and conglomerate fractions of the Lower Cretaceous section. Conglomerate provenance data were collected in the field by tabulating clast composition counts at four positions in the stratigraphic column (Fig. 12). We counted 100 clasts in each of the conglomerate samples, and in order to minimize the uncertainty associated with field identification of lithology, only four major clast types were tabulated (general sedimentary [sandstone, mudstone]; quartzite-carbonate; metamorphic; volcanic). A greater number of sandstone samples were collected and point-counted using the Gazzi-Dickinson method following the procedures of Ingersoll et al. (1984) (Figs. 12 and 13; Table 1).

Two main petrofacies can be recognized from the conglomerates (Fig. 12), a volcanic-sedimentary petrofacies, and a mixed volcanic-sedimentary-metamorphic petrofacies. The lat-

TABLE 1. RAW POINT-COUNT DATA FROM LOWER CRETACEOUS SANDSTONES OF THE ONCH HAYRHAN REGION

Sample	Latitude (N)	Longitude (E)	Q m	Q p	Cht	K	P	Lvm	Lslt	Lm	unid L	bt	ms	chl	heav	cmt	matr
A1	42.05′ 54.2″	104.25′ 48.3″	115	48	4	17	58	140	14	0	1	5			1	19	67
A2	42.05′ 54.2″	104.25′ 48.3″	193	66	6	5	78	108	13	4	2	3	6			4	16
B1	42.05′ 07.8″	104.26′ 05.5″	57	33	48	0	15	63	222	17	11	3				3	28
B2	42.05′ 07.8″	104.26′ 05.5″	75	29	21	1	21	63	128	46						10	102
C1	42.05′ 46.7″	104.26′ 09.9″	96	48	20	13	28	41	16	18	19				4	75	132
D1	42.05′ 05.5″	104.26′ 23.9″	105	51	9	4	29	104	49	40					3	100	2
D2	42.05′ 05.5″	104.26′ 23.9″	73	71	27	1	9	18	29	126					3	48	93
E1	42.04′ 38.9″	104.26′ 26.4″	92	23	5	52	42	104	93	37		4					48
E2	42.04′ 38.9″	104.26′ 26.4″	115	43	8	48	48	87	63	31				5		15	35
E3	42.04′ 38.9″	104.26′ 26.4″	84	47	73	53	45	32	73	2		5			2	71	9
E4	42.04′ 38.9″	104.26′ 26.4″	60	69	111	8	9	93	44	26		5			4	74	12

Note: Point counts were performed using the Gazzi-Dickison method (Ingersoll et al., 1984), with 500 counts per slide. Qm—monocrystalline quartz, Qp—polycrystalline quartz, Cht—chert, K—potassium feldspar, P—plagioclase, Lvm—volcanic and metavolcanic rock fragments, Lslt—sedimentary rock fragments, Lm—metamorphic rock fragments, unid L—undifferentiated rock fragments, bt—biotite, ms—muscovite, chl—chlorite, heav—dense minerals, cmt—cement, matr—matrix. See Figures 4 and 9 for sample locations.

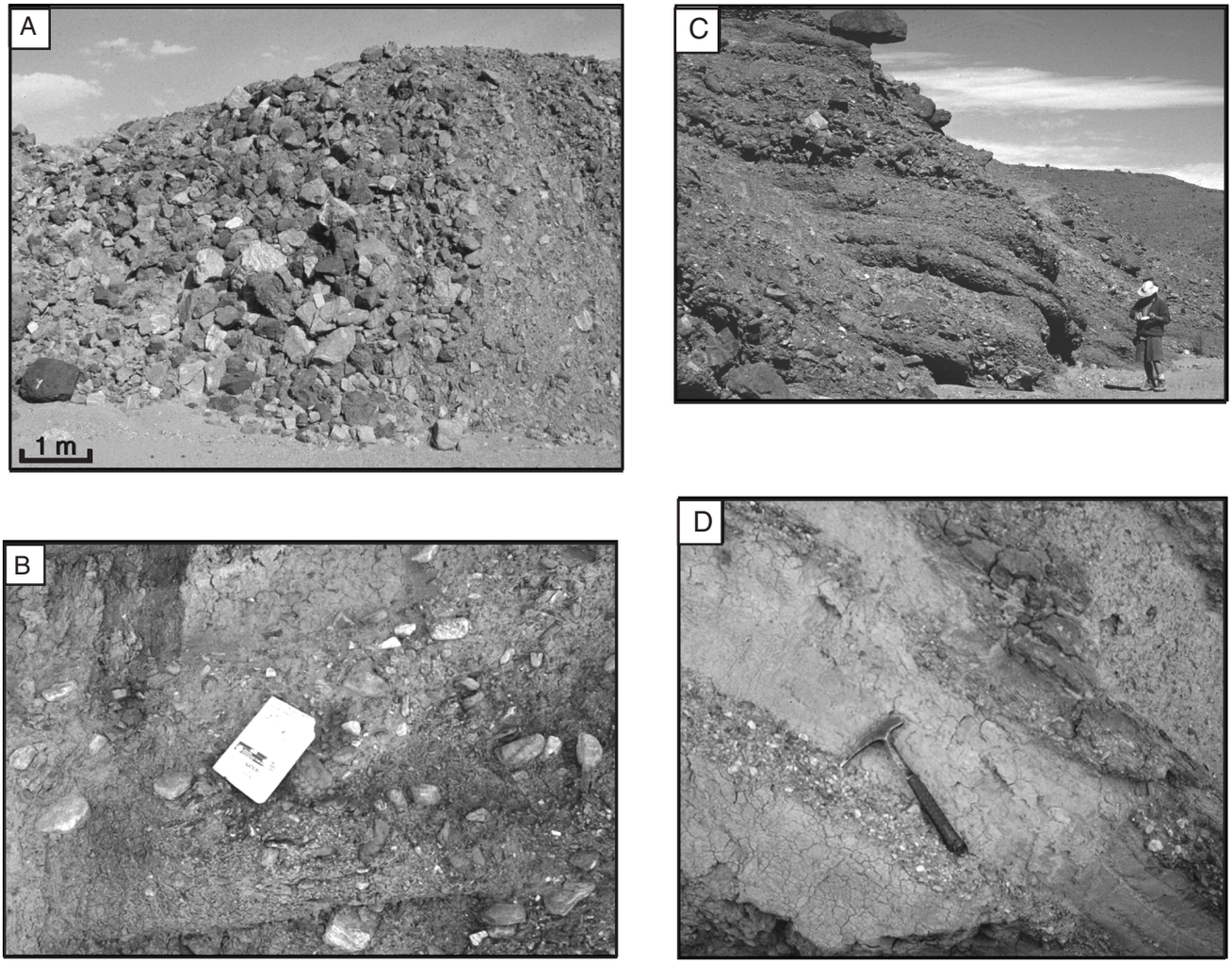

Figure 11. Outcrop photos of typical sedimentary styles of Lower Cretaceous section at Onch Hayrhan. Photos are keyed to detailed sections of Figure 10. A: Unsorted, clast-supported, matrix-free boulder bed, interpreted as talus slope deposit. B: Matrix-supported debris-flow deposit. Field book for scale (12 × 19 cm). C: Conglomerate and sandstone sequence; note large outsized boulders and crude bedding. Person for scale. D: Lenses of moderately rounded pebble conglomerate interstratified with plane- to cross-laminated sandstone and siltstone, interpreted as braided fluvial deposit. Hammer for scale.

ter is especially important, because some of the metamorphic clasts are recognizable as mylonite similar to that exposed in the footwall of the Yagan–Onch Hayrhan core complex (Fig. 14). Other distinctive lithologies include carbonate and quartzite clasts derived from the Permian and older section. Volcanic clasts present in conglomerate and present to abundant in sandstone (Fig. 12) appear to be mostly Paleozoic, rather than Mesozoic and synextensional, based on fabric and degree of alteration (paleovolcanic, rather than neovolcanic in the usage of Zuffa, 1980).

Clast counts, although limited in number, generally show lower percentages of high-grade metamorphic clasts in the younger parts of the stratigraphic section, including the disappearance of mylonitic rock fragments somewhere between sections C and B (Fig. 12). Sandstone point counts from thin sections demonstrate the lithic-rich nature of these samples (Fig. 13). The point counts indicate a comparatively weaker evolutionary trend (Fig. 12), probably reflecting greater dispersal of sand in the environment as well as the difficulty in distinguishing between different types of metamorphic lithologies in medium-grained sand fractions (250–500 μm).

Discussion. The Lower Cretaceous sedimentary section associated with the metamorphic core complex in the Onch Hayrhan area strongly suggests synsedimentary tectonism and structural localization of sediment accumulation. The overall coarse-grained nature of the sequence (Fig. 10), its proximity to

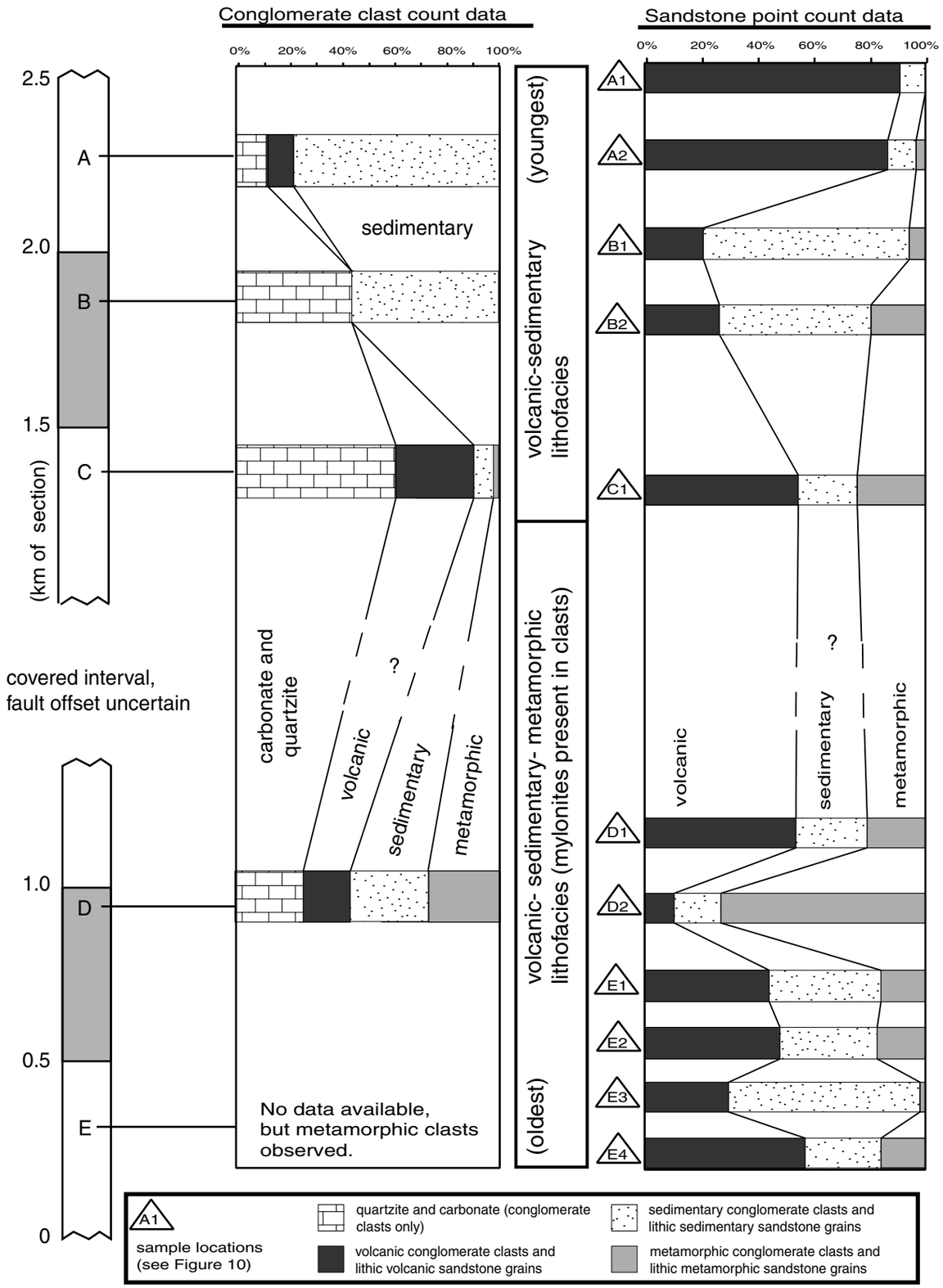

Figure 12. Conglomerate and sandstone clast composition data plotted by stratigraphic position. Sandstone point-count data are recorded in Table 1.

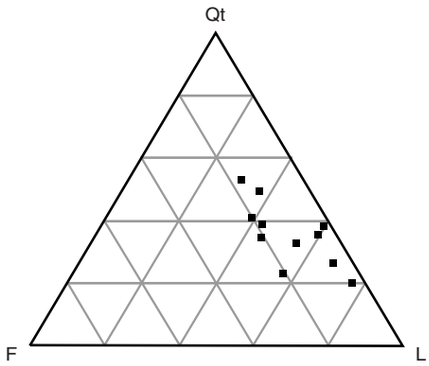

Figure 13. Ternary plot of total framework grains (QtFL) of Lower Cretaceous sandstone. No stratigraphic trends from youngest to oldest samples are evident in QtFL data. See Table 1 for sandstone point-count data.

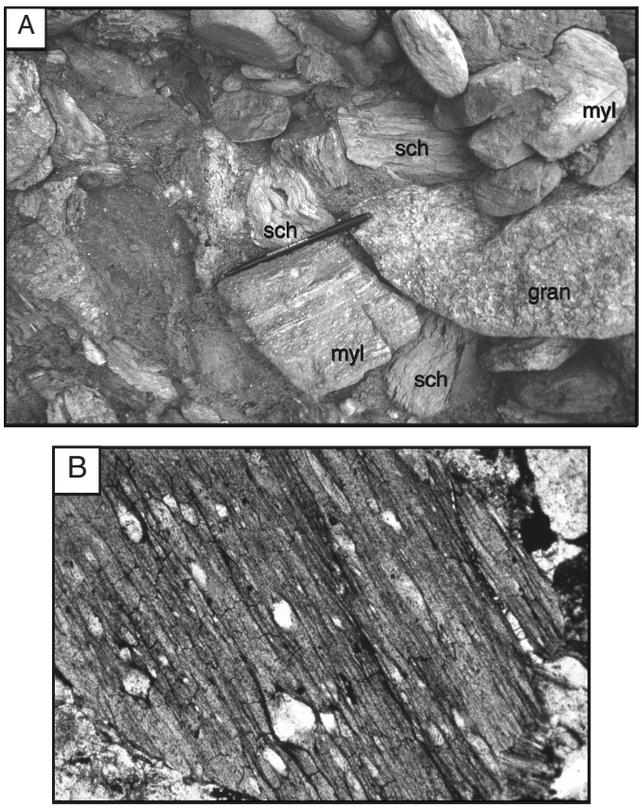

Figure 14. A: Photographs of metamorphic detritus from Lower Cretaceous sequence. Boulder bed from metamorphic petrofacies (lowermost conglomerate sample of Fig. 12). Clasts are predominantly mylonite (myl), schist (sch), and granite (gran). Pen for scale. B: Photomicrograph of coarse sand grain of metamorphic lithic rock, from sample E-1 (Fig. 12). Field of view is ~1 mm across.

probably coeval faults and the transfer zone (Fig. 4), and progressively rotated beds in a fanning-dip pattern (Fig. 9) indicate structurally induced, proximal deposition. Sedimentary units are inferred to be sheetflood dominated (type II alluvial fans of Blair and McPherson, 1994), produced by rapid uplift and intense mechanical erosion of the source area.

General trends in the evolution of depositional systems at Onch Hayrhan are evident from the oldest to youngest stratigraphic sequences (Fig. 10). As shown in section E (Fig. 10), the older parts of the synextensional sequence reflect finer grained, more distal, braided fluvial deposition. Older units grade upsection into extremely coarse, proximal, unsorted alluvial deposits (Figs. 11, A and B). We interpret this shift as recording progradation of an alluvial fan where a more distal braid plain sequence shifts vertically into increasingly proximal middle to upper fan deposits.

The limited size of the provenance data set precludes any firm conclusions regarding evolution of the sediment source terrane. Particularly in the case of proximal sedimentary sequences, conglomerate and sandstone provenance is strongly dependent on source lithologies that crop out in small, localized drainages that may not accurately represent evolution of the system overall (see first-order petrologic models of Ingersoll, 1990). Thus, evolution of the sequence toward increasingly localized drainage of a specific source area in which high-grade metamorphic rocks were not exposed may explain the lack of mylonitic conglomerate pebbles in the younger parts of the section. Metamorphic sand grains that persist throughout the sequence (Fig. 12) probably represent more integrated drainages in the source area, as well as the greater dispersion of sand-sized detritus across the basin.

Mesozoic climate was also an important factor influencing the formation of synextensional sedimentary facies at Onch Hayrhan. Several lines of evidence indicate that southern Mongolia had a relatively wet climate during the Jurassic–Early Cretaceous. Tree-ring analyses from a Late Jurassic petrified forest in the East Gobi basin indicate strong seasonal fluctuations in water supply and possibly a monsoonal climate (Keller and Hendrix, 1997). Jurassic–Cretaceous sedimentary sequences in other parts of the East Gobi basin support the presence of widespread stratified lakes, coal-forming swamps, and soil formation (discussed in the following; Figs. 15–17). Thus, the Cretaceous sedimentary deposits at Onch Hayrhan differ from many of the classic detachment-related basins documented in the western United States because they probably did not form in a dominantly arid environment (Friedmann and Burbank, 1995; exceptions include Muddy Creek half graben, southwest Montana; Janecke et al., 1999). In addition to structural activity in the source area, seasonal changes in water supply likely influenced the preserved sequence at Onch Hayrhan. For example, seasons of high rainfall may have triggered more of the debris-flow units, whereas dry-season sedimentation was probably characterized by rock falls and sheetfloods.

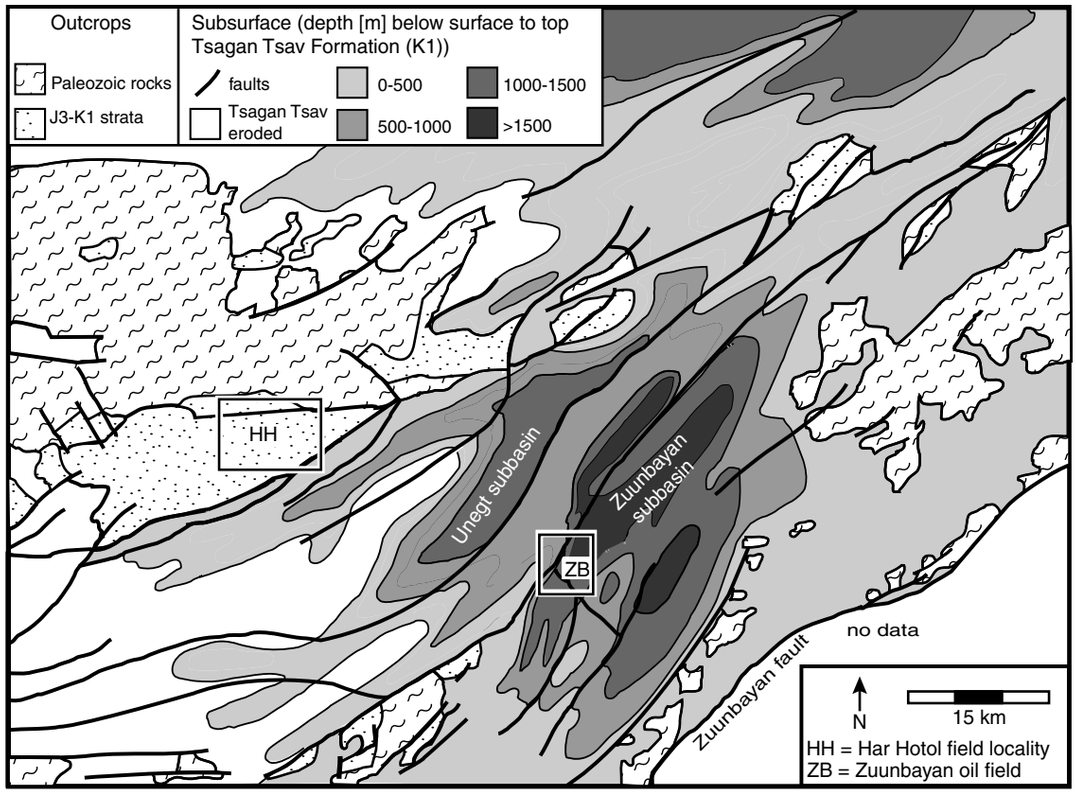

Figure 15. Depth-structure map on Tsagan Tsav (Lower Cretaceous) horizon of Zuunbayan and Unegt subbasins, northeastern East Gobi basin (Shirakov and Kopytchenko, 1983). Shaded contours represent meters below present-day surface to top of Tsagan Tsav Formation, as compiled from seismic, magnetic, and well-log data (Shirakov and Kopytchenko, 1983). See Figure 2 for location.

Unfortunately, we currently lack geochronologic data sufficient to infer sedimentation or unroofing rates. A paucity of ash or other interstratified datable materials in this unfossiliferous section probably renders calculations of rates impossible, but linked thermochronologic study of metamorphic clasts and the metamorphic core complex may eventually shed some light on the timing of structural and/or erosional unroofing and sedimentation rates.

REGIONAL IMPLICATIONS OF THE YAGAN–ONCH HAYRHAN CORE COMPLEX

Strain partitioning and sedimentary basin development in southern Mongolia

The Onch Hayrhan core complex locality represents the high-strain end member of the Mesozoic extensional regime in southern Mongolia. In contrast, the low-strain extensional end member is represented by intracontinental rifting in the area around the Zuunbayan oil field in the northeastern part of the basin (Figs. 2 and 15). Rifting in this part of the basin resulted in the formation of a series of subbasins bounded by high-angle normal faults, as demonstrated by field mapping (Graham et al., 1996; Johnson et al., 1997b), and unpublished reflection seismic data gathered by the petroleum industry. The presence of a detachment fault at depth below these half-grabens cannot be completely discounted; however, proprietary seismic reflection data show no evidence of a regional detachment within ~4 km of the surface.

In addition to the two contrasting structural styles of Mesozoic extension in the East Gobi basin, sedimentary successions associated with each of the structural settings are equally distinctive. We have studied the sedimentary sequences of rifted portions of the East Gobi basin in some detail (Graham et al., 1996; Johnson et al., 1997a), and we briefly summarize that work for comparison with the sedimentary sequence associated with the high-strain extensional regime described at Onch Hayrhan.

The most complete synrift stratigraphic section exposed in the East Gobi basin is located along the northeastern margin of the basin at Har Hotol, near the Zuunbayan oil field (Johnson et al., 1997a; Fig. 15). At this and nearby localities, >2 km of synextensional strata are exposed (Fig. 16). The sequence accumulated between ca. 155–131 Ma. (Late Jurassic–Early Cretaceous) (Graham et al., 1996) and dominantly reflects mature

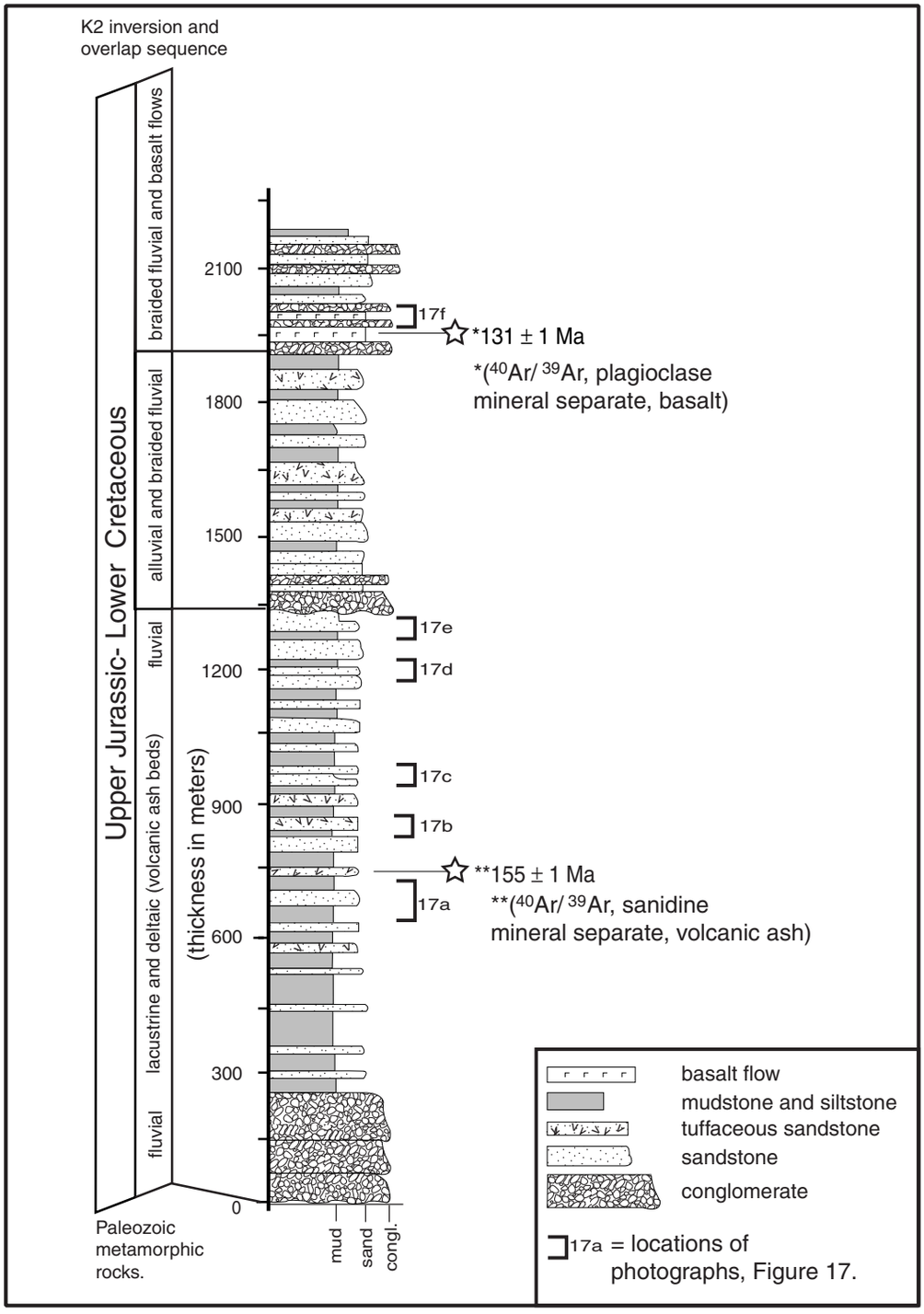

Figure 16. Stratigraphic column and environmental interpretations for Upper Jurassic–Lower Cretaceous syn-rift strata of Har Hotol area. See Figure 15 for location.

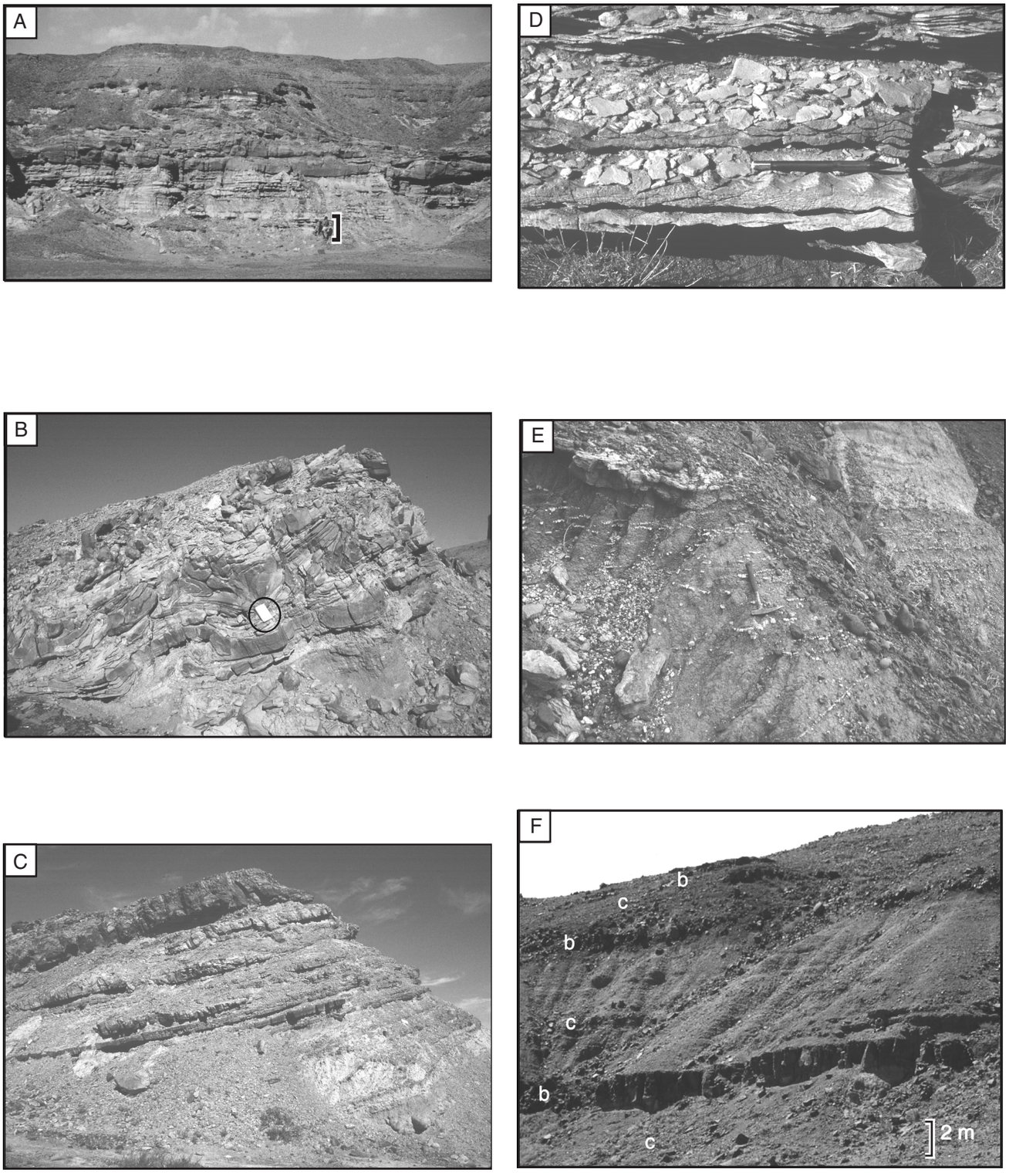

Figure 17. Outcrop photos of typical lithofacies of Har Hotol Upper Jurassic–Lower Cretaceous section. Stratigraphic positions of outcrops are noted in Figure 16. A: Lenticular channel sandstone beds over prodelta mudstones; person at base of cliff for scale. B: Slumping and soft-sediment deformation in fluvial-deltaic sandstone sequence. Field book for scale (12 × 19 cm); C: Upward-thickening sandstone sequence, interpreted as upward shoaling along prograding deltaic lacustrine margin; height of outcrop is ~20 m. D: Lacustrine facies distal to prograding delta margins, including centimeter-scale turbidite layers and symmetric wave ripples; pencil for scale. E: Calcisol development marked by white carbonate nodules within fluvial-alluvial redbed mudstone; hammer for scale. F: Interstratified conglomerate (labeled c) and basalt (labeled b) near top of Har Hotol sequence.

deltaic-fluvial-lacustrine depositional environments and numerous volcanic-ash–dispersal events (Fig. 16).

The basement rocks in this part of the basin are mainly metamorphosed Devonian–Carboniferous volcanic arc sequences (Lamb and Badarch, 1997). Prerift sedimentary rocks are Lower to Middle Jurassic conglomerate, sandstone, and carbonaceous mudstone that unconformably overlie the Paleozoic sequence. The initiation of extension is marked in the synrift stratigraphic sequence by a distinctive ~250-m-thick fluvial conglomerate composed of rounded, imbricated, and mainly basement-derived clasts (0–275 m mark in Fig. 16). This basal conglomerate fines upward abruptly into a siltstone and sandstone unit.

Excellent three-dimensional exposures of this fine-grained unit reveal low aspect-ratio, pervasively slumped, channelized sandstone units capping successive upward-coarsening sequences (Figs. 16 and 17, A–C). We interpret the sequence as a series of prograding lacustrine deltas, which grade laterally into a distal lacustrine sequence. The latter exhibits wave ripples and thin turbidite layers (Fig. 17D). A return to alluvial-fluvial sedimentation occurs in the middle part of the sequence (~1350 m, Fig. 16), with a conglomerate-sandstone redbed section that includes subaerial exposure surfaces and paleosols (Fig. 17E). Fluvially resedimented volcanic ash beds are present throughout much of the upper half of the section, which is capped by multiple interbedded basalt flows, ash layers, and sandstone and conglomerate of braided-fluvial origin (Fig. 17F). A period of structural inversion during mid-Cretaceous time resulted in tilting and erosion of synrift strata, which are overlain by relatively flat lying Upper Cretaceous strata (Fig. 3B).

These stratigraphic studies, combined with our examination of subsurface structure from proprietary seismic lines, indicate that extension along the northeast portion of the East Gobi basin was characterized by high-angle normal faulting and formation of half-graben subbasins. The sedimentary units at Har Hotol compose a typical rift sequence, including multiple ash layers and rapid lateral facies changes from basin-margin alluvial fans to distal, isolated lakes (cf. Friedmann and Burbank, 1995). Sedimentation was dominantly fluvial-lacustrine; limited pulses of conglomerate deposition probably represent initiation and reactivation of normal faults prior to basin inversion. These conglomerate units consist entirely of clasts derived from Paleozoic basement rocks and display tractive structures indicating water working in a braided fluvial depositional system.

Although most of the Jurassic–Cretaceous strata in the East Gobi basin reflect relatively mature, stable fluvial-lacustrine environments in conventional rift systems, as typified by the Zuunbayan–Har Hotol area (Figs. 16 and 17), the southern part of the basin around Onch Hayrhan was subject to large-magnitude, high-strain extension resulting in proximal, rapidly deposited alluvial sequences. Proximal alluvial fan deposits are found in a variety of tectonic settings, and coarse-grained clastic facies are common in classic intracontinental rifts (Gawthorpe et al., 1994; Soreghan et al., 1999), so the presence of these sequences does not specifically require a detachment fault setting. Conversely, fine-grained lacustrine and playa lake deposits have been described in supradetachment basins in the United States (Beratan, 1991; Janecke et al., 1999). However, the distinctive and highly metamorphic provenance of the Onch Hayrhan synextensional deposits, the limited geographic extent of the subbasins, and the overall thickness of the typically coarse, poorly organized, aggradational conglomerate all indicate dramatic uplift of the source area and rapid creation of accommodation space. Combined with our structural data, these deposits appear to represent an extensional setting unique to the southern part of the East Gobi basin.

Thus, the East Gobi basin was segmented into provinces characterized by differences in rate and magnitude of extension, as has been described for the Basin and Range province of the western United States (Faulds and Varga, 1998). The record of strain variation is reflected in the synextensional sedimentary deposits of the basin (cf. Figs. 10 and 16), demonstrating the considerable utility of stratigraphic studies in unraveling this complex extensional system. Strain variations probably were facilitated by transverse transfer zones such as the one we describe in the Onch Hayrhan area (Figs. 4 and 7). In addition, accommodation zones of linked en echelon faults may have helped absorb regional strain variation, a process observed in both the North American Basin and Range (Faulds and Varga, 1998), and the East African Rift (e.g., Ebinger et al., 1987). Although accommodation zones have not specifically been recognized in the East Gobi basin, they may be represented in the subsurface by northwest-southeast–trending (transverse) corridors now covered by the Upper Cretaceous overlap sequence (Fig. 2).

Relation of Mesozoic extension to earlier contractile orogeny

Possible driving mechanisms for Mesozoic–Cenozoic rift-basin formation in east-central Asia include backarc extension west of the Asia-Pacific Cretaceous convergent margin (Watson et al., 1987). In addition, oroclinal closure of the Mongol-Okhotsk ocean (Fig. 18; Zonenshain et al., 1990) may have induced transtension, although the magnitude and timing of this event are poorly documented. We also note that in southernmost Mongolia extension closely followed two important compressional events: (1) closure of the Junggar-Hegen ocean between the North China block and the southern Mongolian arcs at the end of the Permian (Amory et al., 1994; Amory, 1996), and (2) emplacement of north-vergent thrust sheets (Fig. 8) during the Jurassic (Hendrix et al., 1996; Zheng et al., 1996). Recognition of the rapid transition from compressional to extensional tectonics during the middle Mesozoic introduces another possible factor driving regional extension in southern Mongolia: gravitational collapse (Graham et al., 1996).

Mesozoic metamorphic core complexes similar to Yagan–Onch Hayrhan were described by Davis et al. (1996) in the Yinshan-Yanshan belt, by van der Beek et al. (1996) in the Baikal region of southern Siberia (Fig. 18), and by Hacker et al.

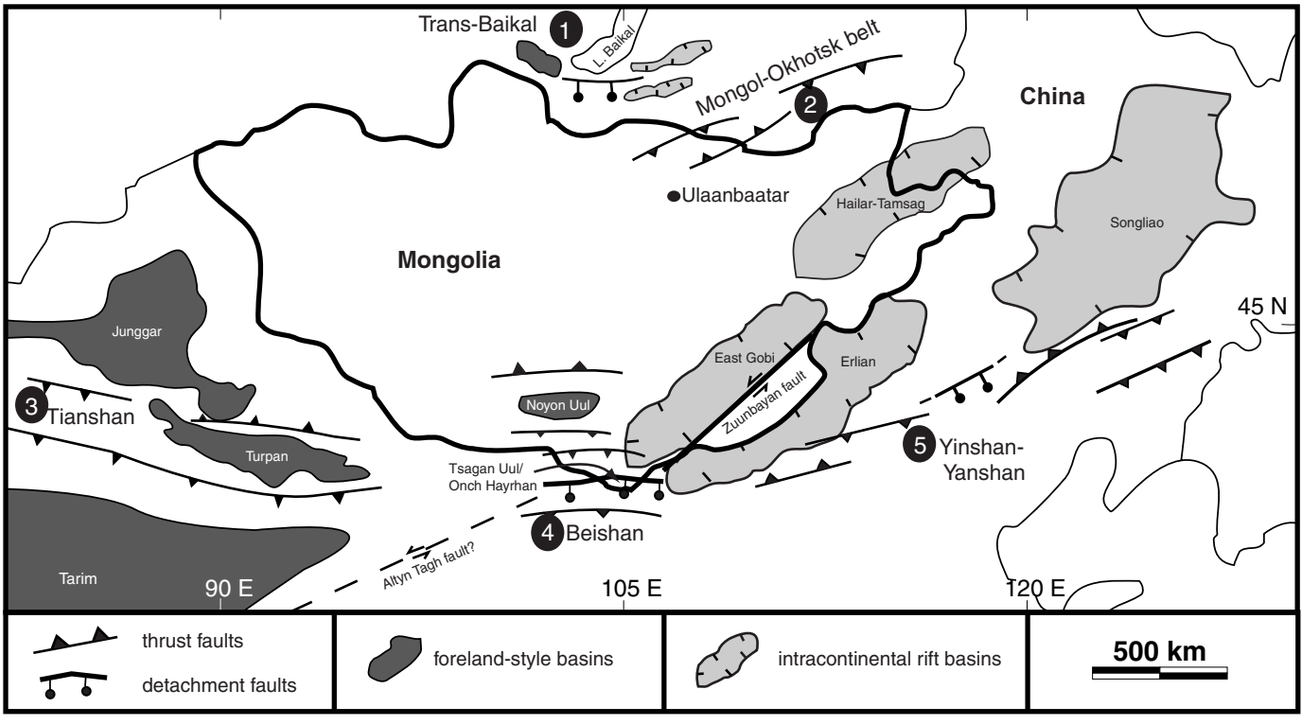

Figure 18. Regional distribution of Mesozoic thrust belts and extensional core complexes and detachment faults (schematic representation). 1, Trans-Baikal region. Late Triassic–Jurassic rift basin initiation, Middle Jurassic inversion, Late Jurassic development of west Baikal foredeep, and Early Cretaceous (140–120 Ma) core complex denudation (van der Beek et al., 1996; cf. Delvaux et al., 1995); 2, Mongol-Okhotsk fold belt. Diachronous west-east closure of Mongol-Okhotsk ocean from Permian to Cretaceous(?) (Zonenshain et al., 1990). 3, Tian Shan. Thrusting and foreland-style basin development, early Mesozoic–Cenozoic (Hendrix et al., 1992). 4, Beishan region. Late Permian–Middle Jurassic(?) thrusting, followed by Middle-Late Jurassic extension and core complex formation (Zheng et al., 1991). 5, Yinshan-Yanshan belt. Jurassic–Cretaceous thrusting and Cretaceous extensional detachment faulting (Davis et al., 1996, 1998a).

(1995) in the Dabie Shan. The association of all of these regions of detachment faulting with preceding episodes of significant crustal shortening suggests a common denominator. Gravitational collapse of overthickened crust underpinning contractile orogenic mountain belts may initiate detachment faulting, as has been suggested for many core complexes and related collapse basins worldwide (Burchfiel et al., 1992; Constenius, 1996). This mechanism also may have been an important factor in the regional segmentation of high- and low-strain extensional provinces of Mesozoic east-central Asia.

The late Mesozoic central Asian extensional province is superposed on an accretionary collage of diverse terranes (Zhang et al., 1984), and thus it provides an interesting comparison to the well-studied U.S. Basin and Range province (Fig. 19). Both examples show similarities in terms of the close timing between periods of shortening and extension, and the formation of both metamorphic core complexes and rift provinces. However, metamorphic core complexes of the western United States formed on long-stabilized Precambrian crust of the North American continent that heated and thickened during Mesozoic arc and/or retroarc tectonism (Graham, 1996). In contrast, highly extended regions in Asia such as the Onch Hayrhan area formed primarily along plate and microplate suture zones, on crust previously thickened during plate collision. Thus, the distribution of these core complexes appears to be strongly controlled by the locations of collisional orogens formed during the tectonic amalgamation of the Asian continent.

CONCLUSIONS

Structural and sedimentary data from the Yagan–Onch Hayrhan metamorphic core complex and from Har Hotol in the East Gobi basin indicate that both high- and low-strain extensional regimes were active during the Early Cretaceous in southern Mongolia. As a result, both a metamorphic core complex and a classic intracontinental rift system are preserved, along with their associated and contemporaneous sedimentary deposits. A transfer fault was partly responsible for locally accommodating strain along the surface termination of the main detachment fault at the Onch Hayrhan metamorphic core complex. Other, unmapped accommodation zones probably helped to partition the high- and low-strain provinces of the East Gobi basin.

Sedimentary sequences at either end of the East Gobi basin also reflect distinct structural settings. Alluvial conglomerate of the Lower Cretaceous Onch Hayrhan section is indicative of rapid, proximal sedimentation driven by large-magnitude ex-

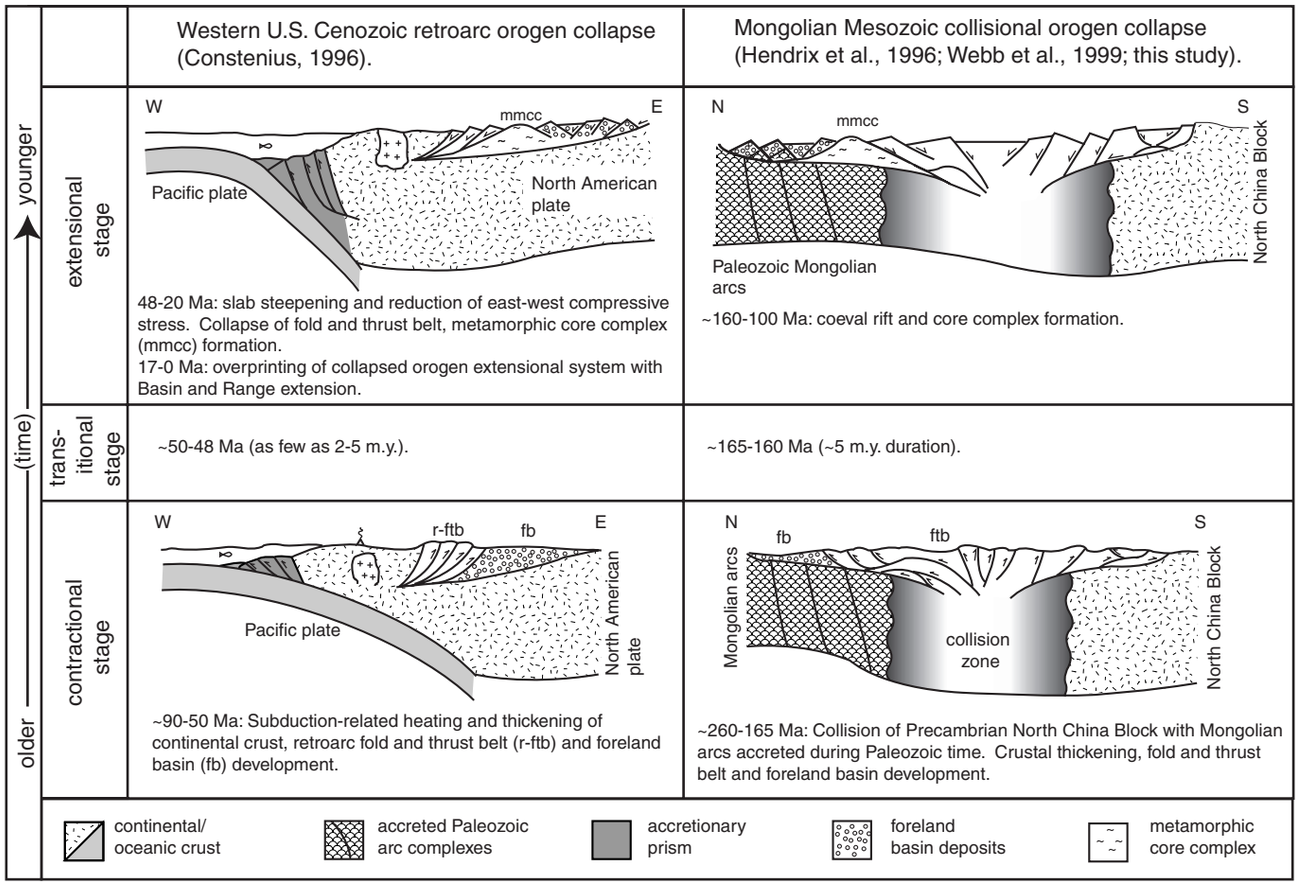

Figure 19. Comparison of contractional, transitional (between final shortening and beginning of extension), and extensional phases of development in Cenozoic of western United States (left column) and Mesozoic of Mongolia (right column). Cross sections are schematic representations only, modeled after Dickinson (1976) and Muñoz (1992).

tension in the area. By comparison, rift sedimentation in the half-graben subbasins near the Zuunbayan oil field was dominantly fluvial-lacustrine and suggestive of longer lived and relatively stable depositional systems.

Regionally, the East Gobi basin is one of several extensional provinces in central Asia that are recognized to have formed immediately following contractional tectonics. The presence of core complexes in many of these areas supports the idea that gravitational collapse of overthickened crust that formed along collisional terrane boundaries may have helped focus regions of high-strain extension during the Mesozoic.

ACKNOWLEDGMENTS

Funding for this project was provided by Nescor Energy and Roc Oil Company, Limited, and by National Science Foundation grants EAR-9708207 and EAR-961455 to S. Graham and M. Hendrix, respectively. C. Johnson was supported by a Gabilan Stanford Graduate Fellowship. We thank Julio Freidman and Kenneth Ridgway, whose comments significantly enhanced the quality of the final manuscript. We also thank A. Chimitsuren and our colleagues at the Mongolian Academy of Sciences, Institute of Geology and Mineral Resources, and the Mongolian Paleontological Institute for their scientific and logistic support.

REFERENCES CITED

Amory, J., 1996, Permian sedimentation and tectonics of southern Mongolia [M.S. thesis]: Stanford, California, Stanford University, 183 p.

Amory, J.Y., Hendrix, M.S., Lamb, M., Keller, A.M., Badarch, G., and Tomurtogoo, O., 1994, Permian sedimentation and tectonics of southern Mongolia: Implications for a time-transgressive collision with north China: Geological Society of America Abstracts with Programs, v. 26, no. 7, p. A-242.

Angelier, J., 1994, Fault slip analysis and palaeostress reconstruction, *in* Hancock, P.L., ed., Continental deformation: Tarrytown, New York, Pergamon Press, p. 53–100.

Baljinnyam, I., Bayasgalan, A., Borisov, B.A., Cisternas, A., Dem'yanovich, M.G., Ganbaatar, L., Kochetkov, V.M., Kurushin, R.A., Molnar, P., Philip, H., and Vaschilov, Y.Y., 1993, Ruptures of major earthquakes and active deformation in Mongolia and its surroundings: Geological Society of America Memoir 181, 62 p.

Beratan, K., 1991, Miocene synextension sedimentation patterns, Whipple Mountains, southeastern California: Implications for the geometry of the Whipple detachment system: Journal of Geophysical Research, v. 96, p. 12425–12442.

Beratan, K., 1998, Structural control of rock-avalanche deposition in the Colorado River extensional corridor, southeastern California–western Arizona, *in* Faulds, J.E., and Stewart, J.H., eds., Accommodation zones and transfer zones: The regional segmentation of the Basin and Range Province: Geological Society of America Special Paper 323, p. 115–125.

Blair, T.C., and McPherson, J.G., 1994, Alluvial fans and their natural distinction from rivers based on morphology, hydraulic processes, sedimentary processes, and facies assemblages: Journal of Sedimentary Research, v. A64, p. 450–489.

Burchfiel, B.C., Chen, Z., Hodges, K., Liu, Y., Royden, L., Deng, C., and Xu, J., 1992, The South Tibetan detachment system, Himalayan Orogen; extension contemporaneous with and parallel to shortening in a collisional mountain belt: Geological Society of America Special Paper 269, 41 p.

Coney, P.J., 1980, Cordilleran metamorphic core complexes; an overview, *in* Crittenden, M.D., Jr., et al., eds., Cordilleran metamorphic core complexes: Geological Society of America Memoir 153, p. 7–31.

Constenius, K.N., 1996, Late Paleogene extensional collapse of the Cordilleran foreland fold and thrust belt: Geological Society of America Bulletin, v. 108, p. 20–39.

Crowell, J.C., 1974, Origin of late Cenozoic basins in southern California, *in* Dickinson, W.R., ed., Tectonics and sedimentation: Society of Economic Paleontologists and Mineralogists Special Publication 22, p. 190–204.

Cunningham, W.D., Windley, B.F., Owen, L.A., Barry, T., Dorjnamjaa, D., and Badamgarav, J., 1997, Geometry and style of partitioned deformation within a late Cenozoic transpressional zone in the eastern Gobi Altai Mountains, Mongolia: Tectonophysics, v. 277, p. 285–306.

Davis, G., Xianglin, Q., Zheng, Y., Tong, H., Yu, H., Wang, C., Gehrels, G., Shafiquallah, M., and Fryxell, J., 1996, Mesozoic deformation and plutonism in the Yunmeng Shan: A metamorphic core complex north of Beijing, China, *in* Yin, A., and Harrison, M., eds., The Tectonic Evolution of Asia: Cambridge, Cambridge University Press, p. 253–280.

Davis, G.A., Cong, W., Zheng, Y., Zhang, J., Zhang, C., and Gehrels, G.E., 1998a, The enigmatic Yinshan fold-and-thrust belt of northern China; new views on its intraplate contractional styles: Geology, v. 26, p. 43–46.

Davis, G.A., Yadong, Z., Cong, W., Darby, B.J., Changhou, Z., and Gehrels, G., 1998b, Geometry and geochronology of Yanshan belt tectonics: Collected works of international symposium on geological science: Beijing, China, Peking University, p. 275–292.

Davis, G.A., Zheng Yadong, Wang Cong, Darby, B.J., and Hua, Yonggang, 1998c, Geologic introduction and field guide to the Daqing Shan thrust, Daqing Shan, Nei Mongol, China: Hohhot, China, Nei Mongol Bureau of Geology and Mineral Resources, Yinshan-Yanshan major thrust and nappe structures field conference, May 8–11, Hohhot, Nei Mongol, China, 23 p.

Delvaux, D., Moeys, R., Stapel, G., Melnikov, A., and Ermikov, V.Y.V., 1995, Palaeostress reconstructions and geodynamics of the Baikal region, Central Asia; Part I, Palaeozoic and Mesozoic pre-rift evolution: Tectonophysics, v. 252, p. 61–101.

Dickinson, W.R., 1976, Plate tectonic evolution of sedimentary basins, *in* Dickinson, W.R., and Yarborough, H., eds., Plate tectonics and hydrocarbon accumulation: American Association of Petroleum Geologists Continuing Education Course Note Series 1, p. 1–62.

Duebendorfer, E.M., and Wallin, E.T., 1991, Basin development and syntectonic sedimentation associated with kinematically coupled strike-slip and detachment faulting, southern Nevada: Geology, v. 19, p. 87–90.

Ebinger, C.J., Rosendahl, B.R., and Reynolds, D.J., 1987, Tectonic model of the Malawi rift, Africa: Tectonophysics, v. 141, p. 215–235.

Faulds, J.E., and Varga, R.J., 1998, The role of accommodation zones and transfer zones in the regional segmentation of extended terranes, *in* Faulds, J.E., and Stewart, J.H., eds., Accommodation zones and transfer zones: The regional segmentation of the Basin and Range Province: Geological Society of America Special Paper 323, p. 1–45.

Friedmann, J.S., and Burbank, D.W., 1995, Rift basins and supradetachment basins: Intracontinental extensional end members: Basin Research, v. 7, p. 109–127.

Gawthorpe, R.L., Fraser, A.J., and Collier, R.E., 1994, Sequence stratigraphy in active extensional basins: Implications for the interpretation of ancient basin-fills: Marine and Petroleum Geology, v. 11, p. 642–658.

Graham, S.A., 1996, Controls on intracontinental deformation in central Asia: Geological Society of America Abstracts with Programs, v. 28, no. 7, p. A-112.

Graham, S.A., Hendrix, M.S., Wang, L.B., and Carroll, A.R., 1993, Collisional successor basins of western China: Impact of tectonics inheritance of sand composition: Geological Society of America Bulletin, v. 105, p. 323–344.

Graham, S.A., Hendrix, M.S., Badarch, G., and Badamgarav, D., 1996, Sedimentary record of transition from contractile to extensional tectonism, Mesozoic, southern Mongolia: Geological Society of America Abstracts with Programs, v. 28, no. 7, p. A-68.

Hacker, B., Ratschbacher, L., and Webb, L., 1995, What brought them up? Exhumation of the Dabie Shan ultrahigh-pressure rocks: Geology, v. 23, p. 743–746.

Hendrix, M.S., Graham, S.A., Carroll, A.R., Sobel, E., McKnight, C.L., Schulein, B.S., and Wang, Z., 1992, Sedimentary record and climatic implications of recurrent deformation in the Tian Shan: Evidence from Mesozoic strata of the north Tarim, South Junggar, and Turpan basins, northwest China: Geological Society of America Bulletin, v. 104, p. 53–79.

Hendrix, M.S., Graham, S.A., Amory, J.Y., and Badarch, G., 1996, Noyon Uul syncline, southern Mongolia; lower Mesozoic sedimentary record of the tectonic amalgamation of Central Asia: Geological Society of America Bulletin, v. 108, p. 1256–1274.

Ingersoll, R.V., 1990, Actualistic sandstone petrofacies; discriminating modern and ancient source rocks: Geology, v. 18, p. 733–736.

Ingersoll, R.V., Bullard, T.F., Ford, R.L., Grimm, J.P., Pickle, J.D., and Sares, S.W., 1984, The effect of grain size on detrital modes: A test of the Gazzi-Dickinson point-counting method: Journal of Sedimentary Petrology, v. 54, p. 103–116.

Janecke, S., McIntosh, W., and Good, S., 1999, Testing models of rift basins: Structure and stratigraphy of an Eocene-Oligocene supradetachment basin, Muddy Creek half graben, south-west Montana: Basin Research, v. 11, p. 143–165.

Jerzykiewicz, T., and Russell, D.A., 1991, Late Mesozoic stratigraphy and vertebrates of the Gobi Basin: Cretaceous Research, v. 12, p. 345–377.

Johnson, C., Graham, S., Webb, L., Hendrix, M., Badarch, G., Sjostrom, D., Beck, M., and Lenegan, R., 1997a, Sedimentary response to Late Mesozoic extension, southern Mongolia: Eos (Transactions, American Geophysical Union), v. 78, p. F175.

Johnson, C.L., Graham, S.A., Hendrix, M.S., and Badarch, G., 1997b, Sedimentary record of Jurassic-Cretaceous rifting, southeastern Mongolia: Implications for the Mesozoic tectonic evolution of central Asia: Geological Society of America Abstracts with Programs, v. 29, no. 6, p. A-228.

Keller, A.M., and Hendrix, M.S., 1997, Paleoclimatologic analysis of a Late Jurassic petrified forest, southeastern Mongolia: Palaios, v. 12, p. 282–291.

Lamb, M.A., and Badarch, G., 1997, Paleozoic sedimentary basins and volcanic-arc systems of southern Mongolia; new stratigraphic and sedimentologic constraints: International Geology Review, v. 39, p. 542–576.

Lamb, M.A., Hanson, A.D., Graham, S.A., Badarch, G., and Webb, L.E., 1999, Left-lateral sense offset of Upper Proterozoic to Paleozoic features across the Gobi Onon, Tost, and Zuunbayan faults in southern Mongolia and implications for other central Asian faults: Earth and Planetary Science Letters, v. 173, p. 183–194.

Lin Chansong, Li Sitian, Wan Yongxian, Ren Jangye, and Zhang Yanmei, 1997, Depositional systems, sequence stratigraphy and basin filling evolution of Erlian fault lacustrine basin, northeast China, *in* Lia Baojun and Li Sitian, eds., Basin analysis, global sedimentology, geology, and sedimentology, Proceedings of the 30th International Geological Congress: VSP, Utrecht, The Netherlands, p. 163–175.

Muñoz, J.A., 1992, Evolution of a continental collision belt: ECORS-Pyrenees crustal balanced cross-section, *in* McClay, K.R., ed., Thrust tectonics: London, Chapman and Hall, 447 p.

Passchier, C.W., and Trouw, R.A.J., 1996, Microtectonics: New York, Springer, 289 p.

Pavlova, E.E., Manankov, I.N., Morozova, I.P., Solovjeva, M.N., Suetenko, O.D., and Bogoslovskaya, M.F., 1991, Permian invertebrates of southern Mongolia: Joint Soviet-Mongolian Paleontological Expedition Transactions, v. 40, 173 p.

Ruzhentsev, S.V., Pospelov, I.I., and Badarch, G., 1989, Tectonics of the Mongolian Indosinides: Geotectonics, v. 23, p. 476–486.

Şengör, A.M.C., Natal'in, B.A., and Burtman, V.S., 1993, Evolution of the Altaid tectonic collage and Palaeozoic crustal growth in Eurasia: Nature, v. 364, p. 299–307.

Shirokov, V.Y., and Kopytchenko, V.N., 1983, Schematic geologic-structure map of the Unegt and Zuunbayan basins, *in* Analysis and summary of geological and geophysical materials on possibility of oil and gas-bearing basins of Mongolia, Volume 1, book 1: Moscow, All-Union Export and Import Corporation, 291 p.

Shuvalov, V.F., 1968, More information about the Upper Jurassic and Lower Cretaceous in the southeastern Mongolia Altai: Academy of Sciences, USSR, Doklady, Earth Sciences Section, v. 179, p. 31–33.

Shuvalov, V.F., 1975, Stratigraphy of Mesozoic deposits of central Mongolia, *in* Zaitsev, N.S., Luwsandansan, B., Martinson, G.G., Menner, V.V., Pavlova, T.G., Peive, A.V., Timfeev, P.P., Tumortogoo, O., and Yanshin, A.L., Stratigraphy of Mesozoic deposits of Mongolia: Transactions of the joint Soviet-Mongolia scientific research geological expedition, v. 13, p. 50–112.

Soreghan, M.J., Scholz, C.A., and Wells, J.T., 1999, Coarse-grained, deep-water sedimentation along a border fault margin of Lake Malawi, Africa: Seismic stratigraphic analysis: Journal of Sedimentary Research, v. 69, p. 832–846.

Suvorov, A.I., 1982, Strukturnyy plan i razlomy territorii Mongolii: Izvestiya Akademii Nauk SSSR, Seriya Geologicheskaya, v. 1982, p. 122–136.

Traynor, J.J., and Sladen, C., 1995, Tectonic and stratigraphic evolution of the Mongolian People's Republic and its influence on hydrocarbon geology and potential: Marine and Petroleum Geology, v. 12, p. 35–52.

van der Beek, P., Delvaux, D., Andriessen, P., and Levi, K., 1996, Early Cretaceous denudation related to convergent tectonics in the Baikal region, SE Siberia: Geological Society of London Journal, v. 153, p. 515–523.

Watson, M.P., Hayward, A.B., Parkinson, D.N., and Zhang, Z.M., 1987, Plate tectonic history, basin development and petroleum source rock deposition onshore China: Marine and Petroleum Geology, v. 4, p. 205–225.

Webb, L., Graham, S., Badarch, G., Johnson, C., Hendrix, M., Beck, M., Sjostrom, D., and Lenegan, R., 1997, Characteristics and implications of the Onch Hayrhan metamorphic core complex of southern Mongolia: Eos (Transactions, American Geophysical Union), v. 78, p. F174.

Webb, L.E., Graham, S.A., Johnson, C.L., Badarch, G., and Hendrix, M.S., 1999, Occurrence, age, and implications of the Yagan-Onch Hayrhan metamorphic core complex, southern Mongolia: Geology, v. 27, no. 2, p. 143.

Yanshin, A.L., 1989, Map of geological formations of the Mongolian People's Republic: Moscow, Academia Nauka USSR, scale 1:1 500 000.

Yue, Y., and Liou, J.G., 1999, Two stage evolution model for the Altyn Tagh fault, China: Geology, v. 27, p. 227–230.

Zhang, Z., Liou, J.G., and Coleman, R., 1984, An outline of the plate tectonics of China: Geological Society of America Bulletin, v. 95, p. 295–312.

Zheng, Y., and Zhang, Q., 1993, The Yagan metamorphic core complex and extensional detachment fault in Inner Mongolia: Acta Geologica Sinica, v. 67, p. 301–309.

Zheng, Y., Wang, S., and Wang, Y., 1991, An enormous thrust nappe and extensional metamorphic core complex in Sino-Mongolian boundary area: Science in China, ser. B, v. 34, p. 1145–1152.

Zheng, Y., Zhang, Q., Wang, Y., Liu, R., Wang, S.G., Zuo, G., Wang, S.Z., Lkaasuren, B., Badarch, G., and Badamgarav, Z., 1996, Great Jurassic thrust sheets in Beishan (North Mountains); Gobi areas of China and southern Mongolia: Journal of Structural Geology, v. 18, p. 1111–1126.

Zonenshain, L.P., Markova, N.G., and Nagibina, M.S., 1971, Relationship between the Paleozoic and Mesozoic structures of Mongolia: Geotectonics, v. 4, p. 229–233.

Zonenshain, L., Kuzmin, M., Natapov, L., and Page, B., 1990, Geology of the USSR: A plate tectonic synthesis: American Geophysical Union Geodynamics Series, v. 21, 242 p.

Zuffa, G.G., 1980, Hybrid arenites: Their composition and classification: Journal of Sedimentary Petrology, v. 50, p. 21–29.

Manuscript Accepted by the Society June 5, 2000

Printed in the U.S.A.